Soft X-ray Absorption Spectroscopy

Kenta Amemiya (KEK-PF)

1. Advantages and Disadvantages of
   Soft X-ray Absorption Spectroscopy (SXAS)
2. SXAS studies on Surface and Thin films
3. Novel SXAS Techniques
   3-1. Depth-resolved XAS
   3-2. Wavelength-dispersive XAS

Soft X-ray Absorption Spectroscopy (~100-4000 eV)

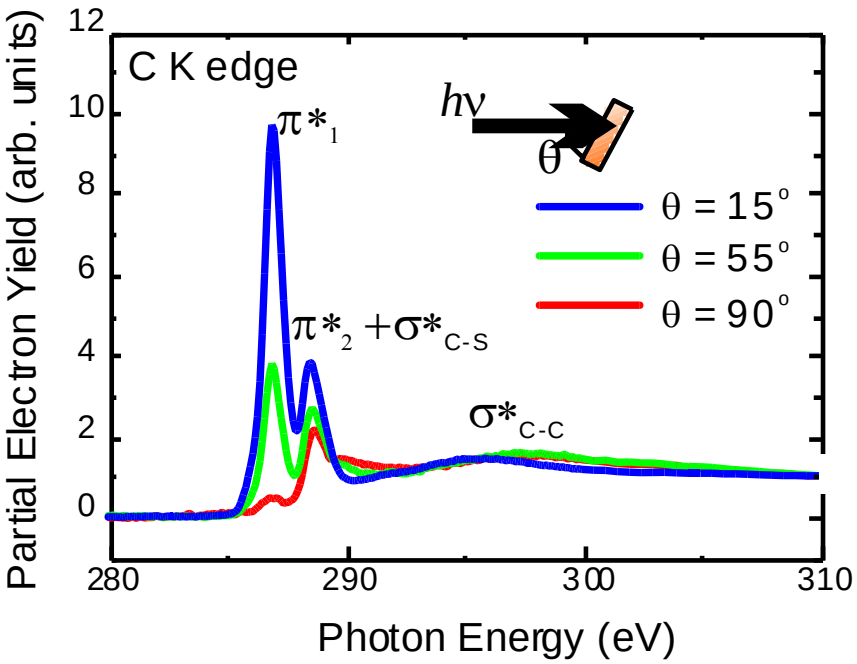

1. Element Selectivity
   <- Core-hole excitation (1s, 2p…)
   (C: 290 eV, N: 400 eV, O: 530 eV…)
2. Information on Chemical Species
   <- Characteristic peaks (π*, σ*…)
3. Structural information (bond length…)
   EXAFS (Extended X-ray Absorption Fine Structure)
4. Information on Anisotropy
   <- Linear polarization
   (molecular orientation, lattice distortion)
5. Magnetic information
   <- Circular polarization
6. High Sensitivity

In the Soft X-ray region,

1. Vacuum condition is normally required. (NOT ultra-high vacuum)
   Special sample cell or He atmosphere is available for ambient pressure.
2. Surface sensitive
   several nm for electron yield, ~0.1 μm for fluorescence yield

XAS Measurement in the Soft X-ray Region

3 ML Fe / Cu(100) Fe L-edge XAS

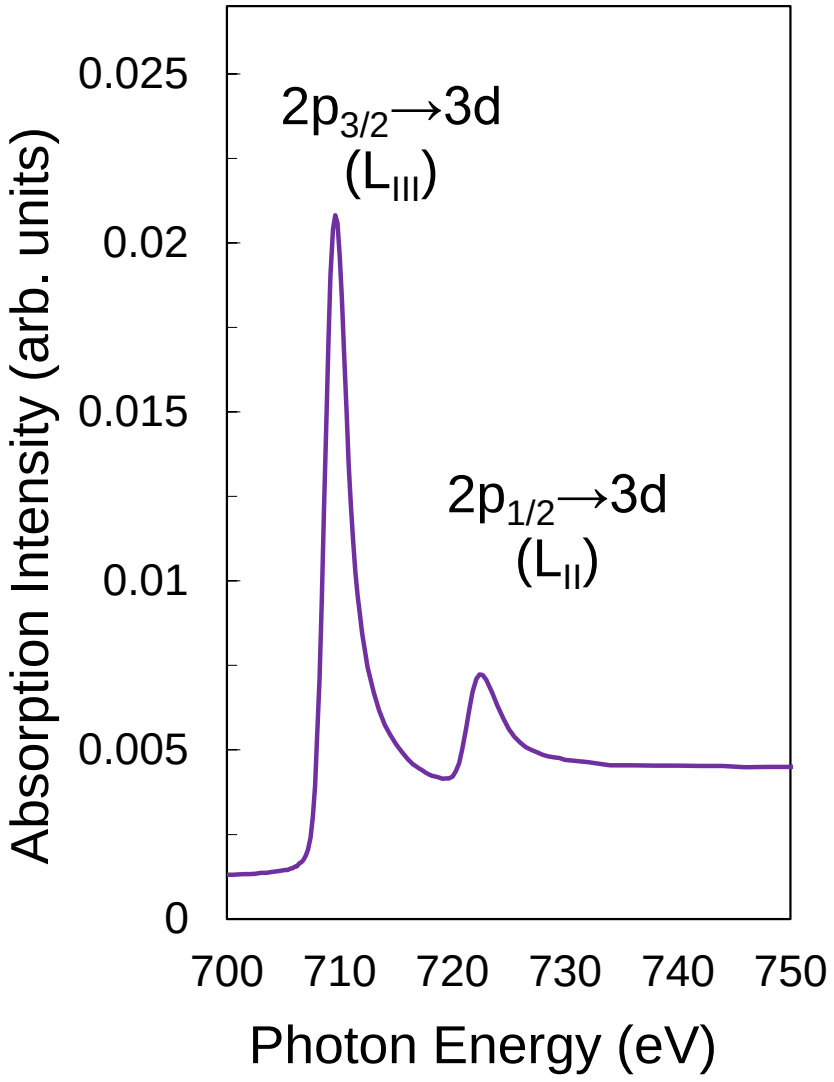

How can we measure

X-ray absorption spectrum ?

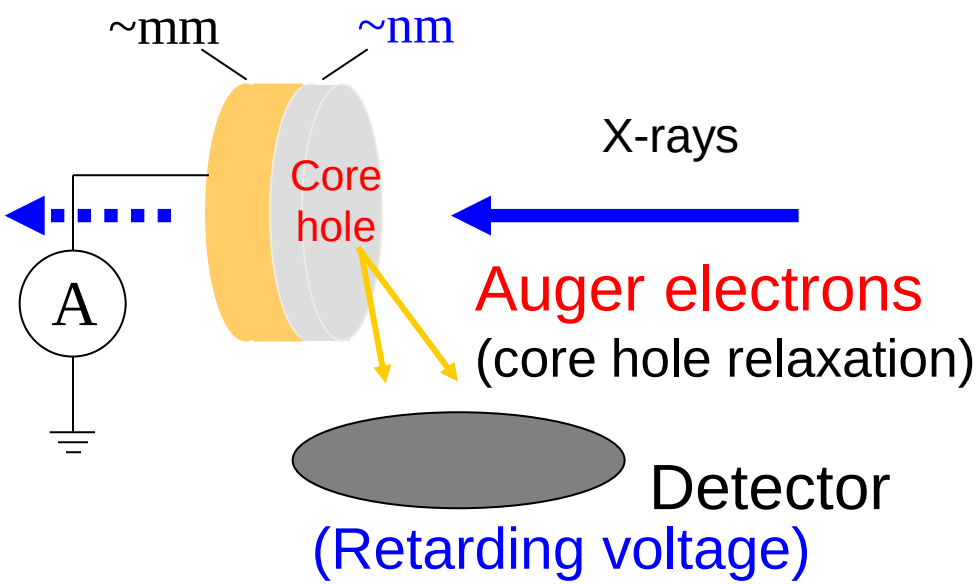

Electron yield XAS

Total electron yield (TEY)

Partial electron yield (PEY)

cf. Fluorescence yield (FY)

Advantages and Disadvantages of SXAS

Short Penetration Length

Transmission mode can be available only for very thin samples
with very thin or no substrate.

Electron yield mode is usually adopted because of high efficiency.
Special care is necessary for insulators (powders might be OK).

Fluorescence yield efficiency is very small for light elements.
<1 % for C, N, O
Be careful for the self absorption (saturation) effect.

Samples should be usually kept in vacuum (NOT ultra-high vacuum).
Some attempts have been made to realize ambient-pressure
or liquid-state measurements.

Surface Sensitive

Sub-monolayer samples can be investigated.

Bulk information is hardly obtained, especially in the electron yield mode.

Sensitive to Electronic and Magnetic States of light elements

Valence electrons can be directly investigated by 1s->2p excitation of C, N, O,… and 2p->3d excitation of 3d transition metals.

Absorption Edges in the Soft X-ray Region

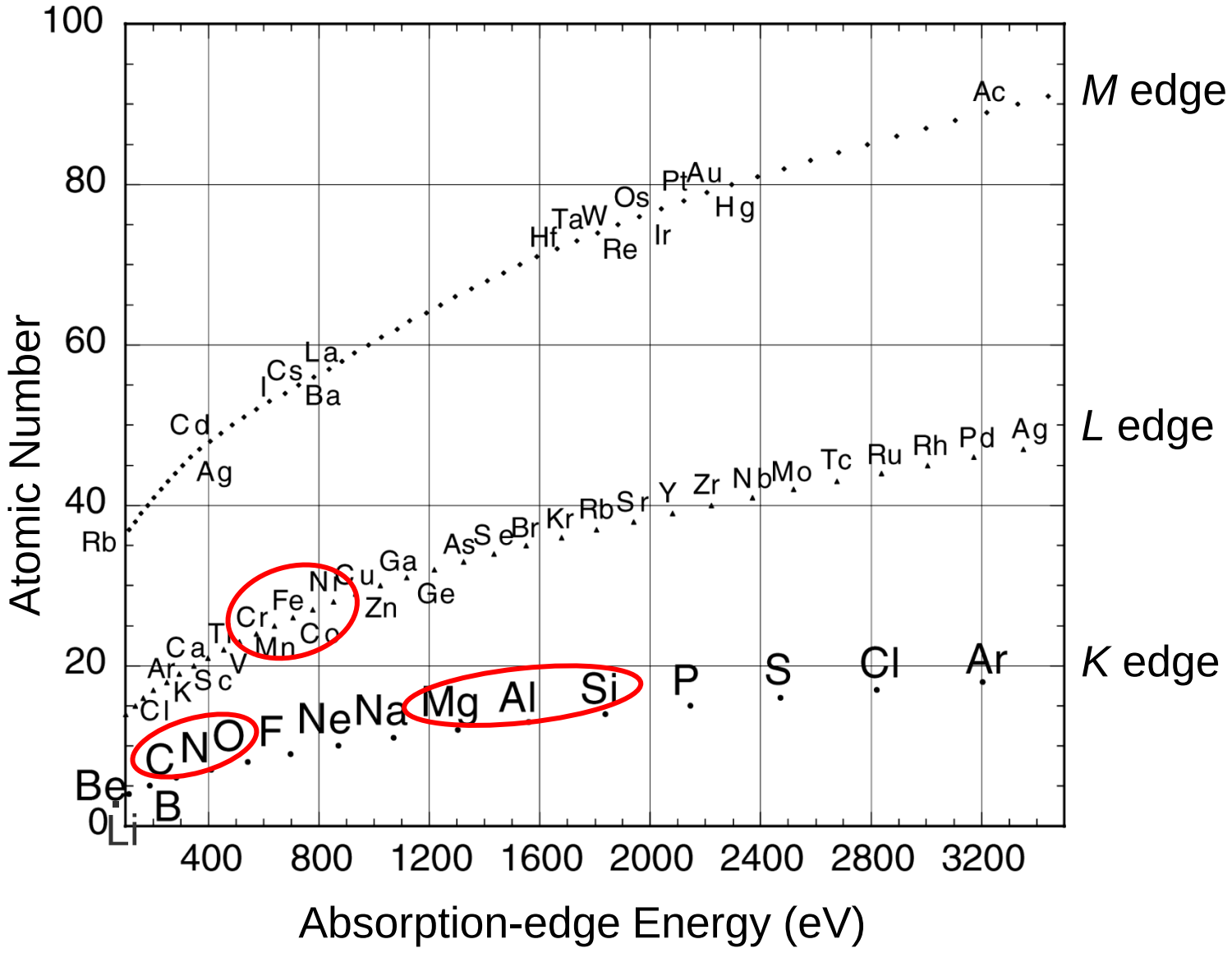

1. Advantages and Disadvantages of

   Soft X-ray Absorption Spectroscopy (SXAS)

2. SXAS studies on Surface and Thin films

3. Novel SXAS Techniques

   3-1. Depth-resolved XAS

   3-2. Wavelength-dispersive XAS

Near-edge Spectroscopy

Near-edge X-ray Absorption Fine Structure (NEXAFS)
X-ray Absorption Near-edge Structure (XANES)

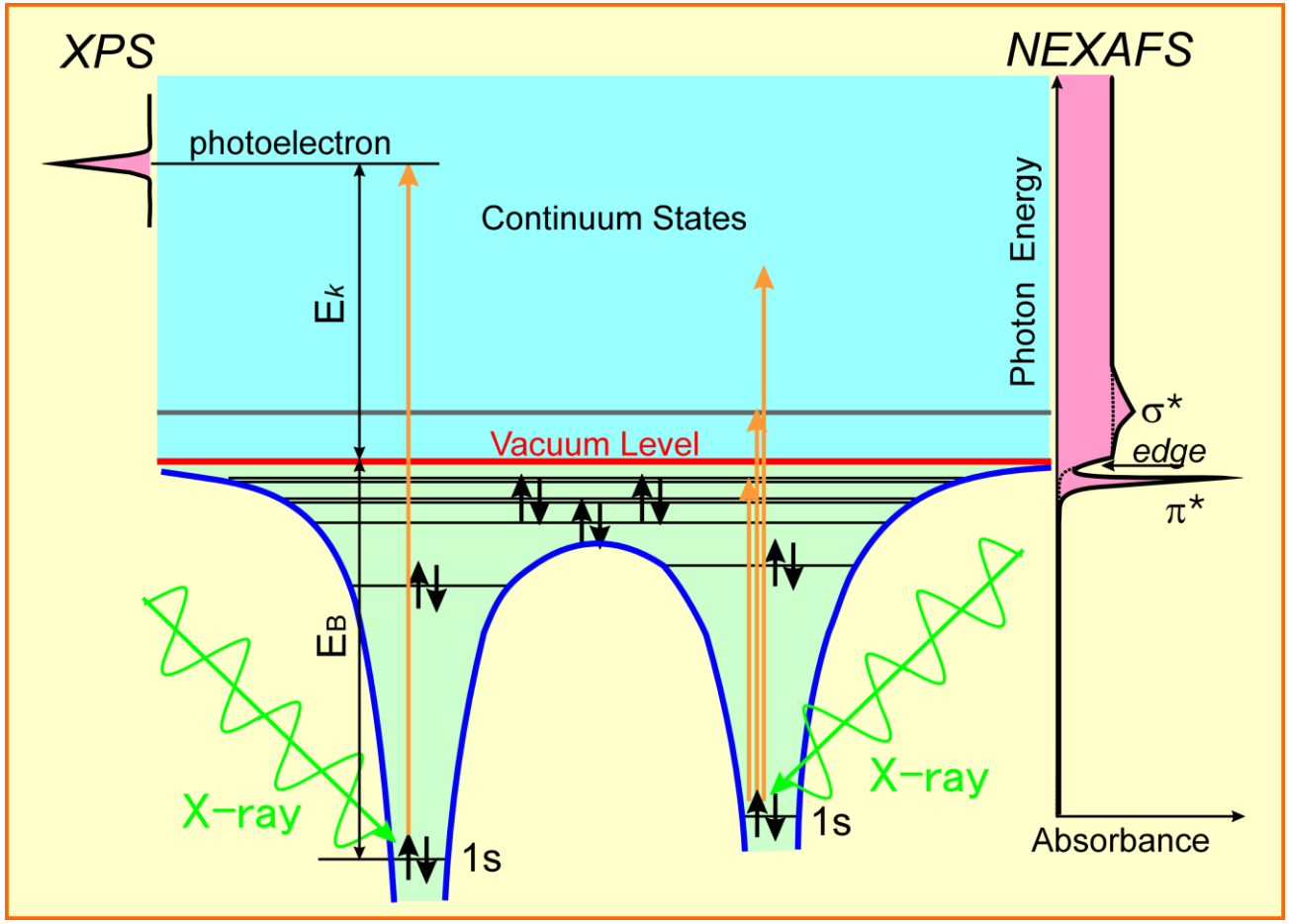

Chemical species

Structural information (orientation)

Near-edge Spectroscopy

Determination of Chemical Species

Initial oxidation process of Si

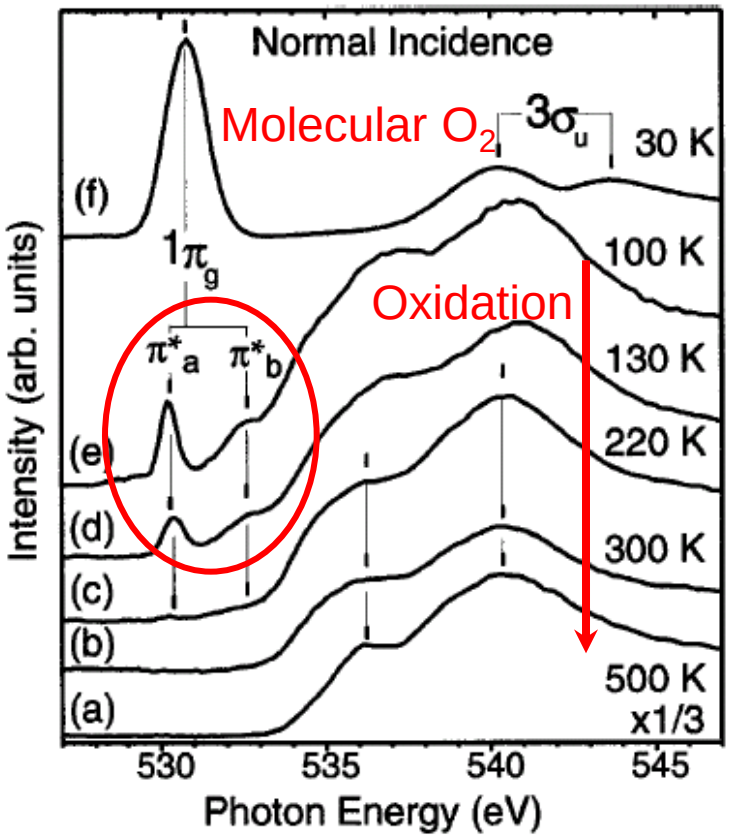

Existence of molecular oxygen
in the initial stage of Si oxidation

Matsui et al., Phys. Rev. Lett. **85,** (2000) 630.

Thiophene (C_4H_4S) molecule on Au(111)

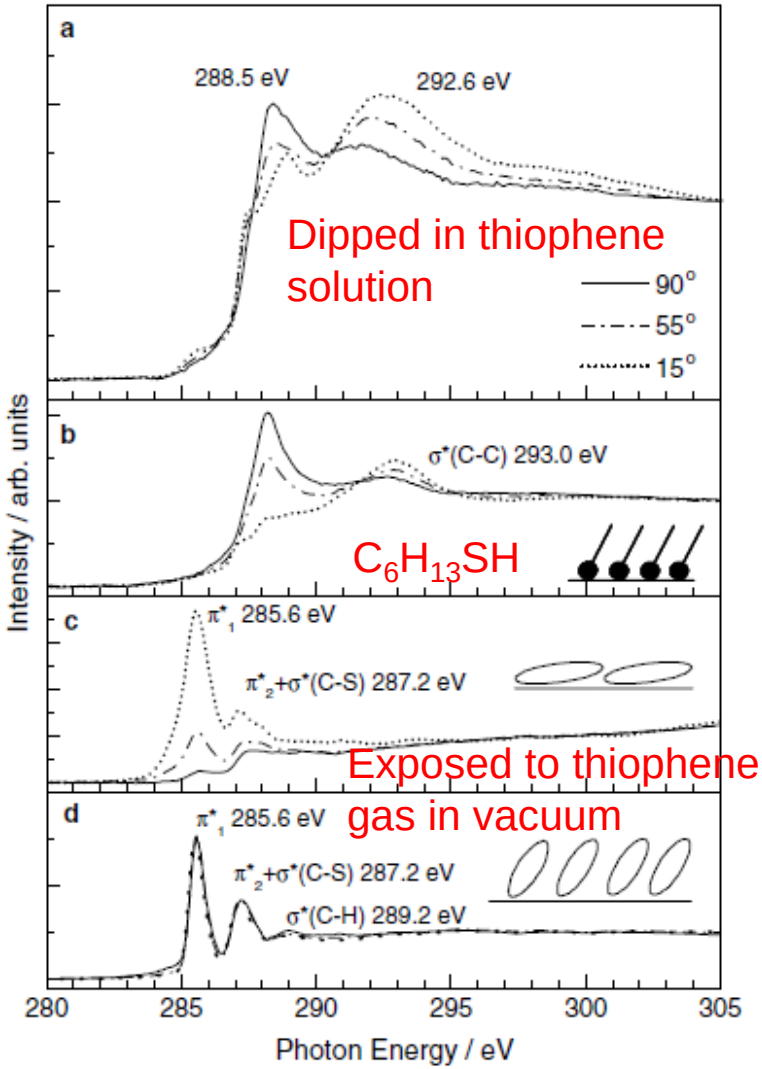

Different chemical species depending
on preparation processes

Sako et al., Chem. Phys. Lett. **413,** (2005) 267.

Determination of Atomic Structure

Extended X-ray Absorption Fine Structure (EXAFS)

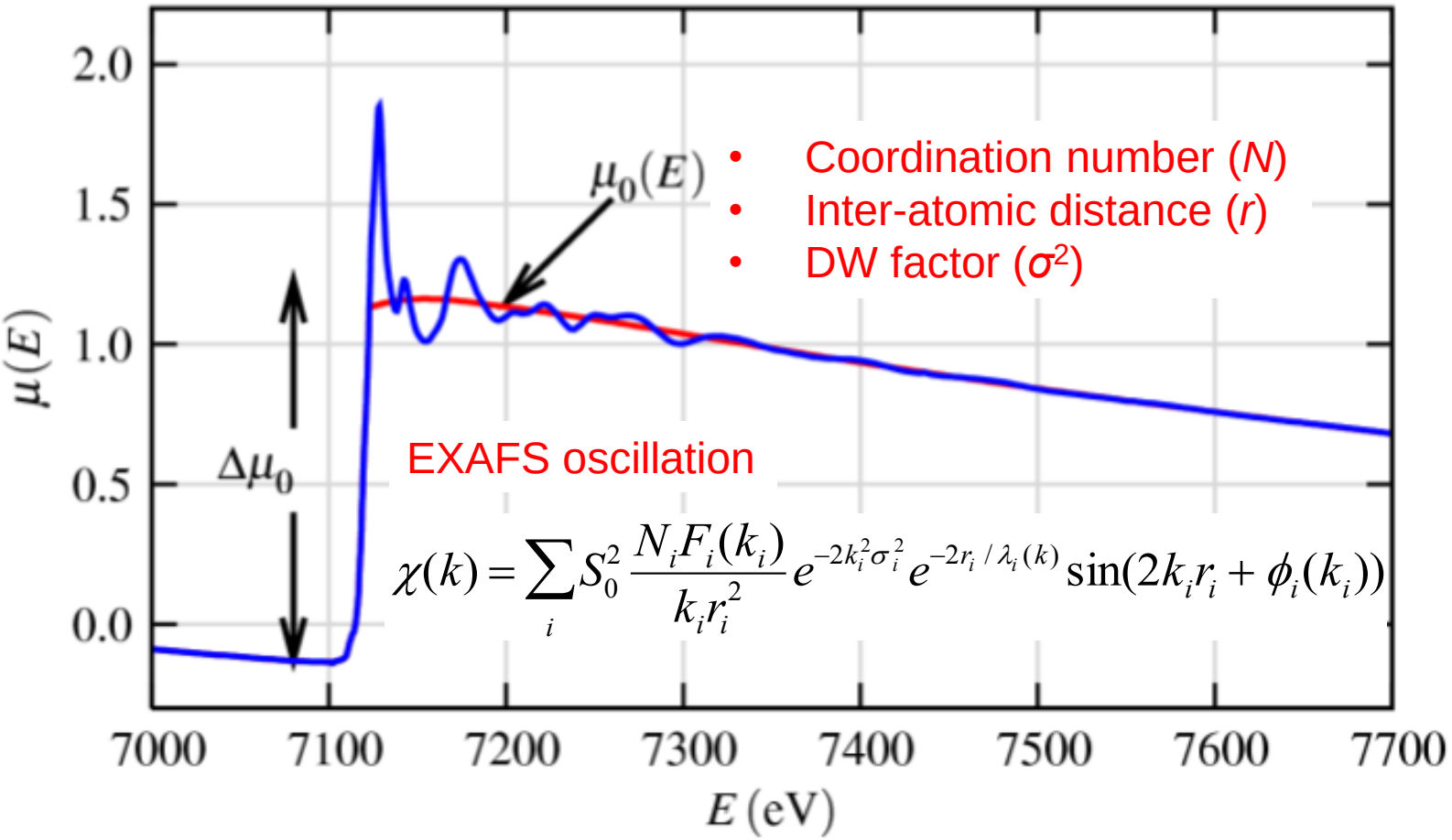

Fe *K*-edge XAFS spectrum $\mu(E)$ of FeO

Determination of Atomic Structure

Amemiya et al., Phys. Rev. B **59,** (1999) 2307.

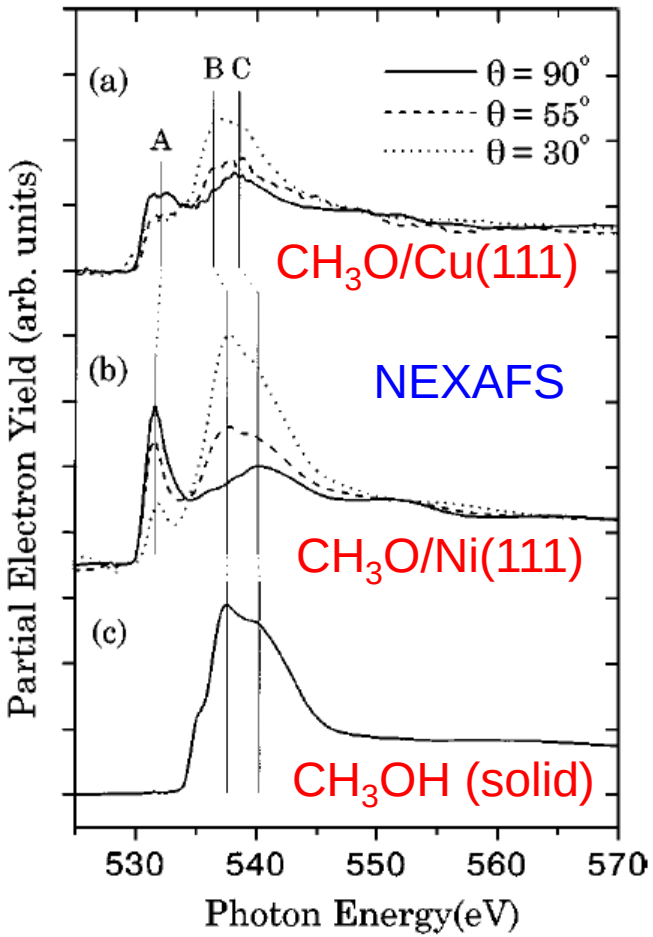

Peak B ($1s \rightarrow \sigma^*_{CO}$) -> C-O bond length

Angle (θ) dependence -> molecular orientation

Application to surface molecule (CH_3O)

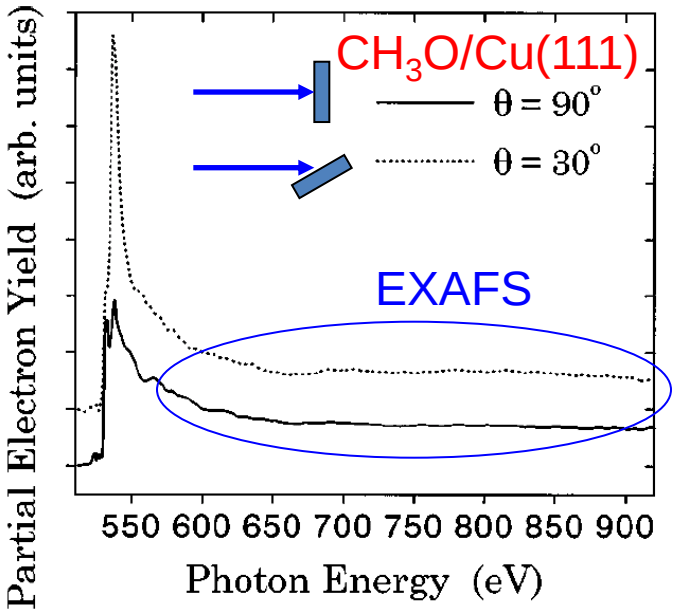

Oscillation period -> O-Cu bond length

Angle (θ) dependence -> bond angle

adsorption site

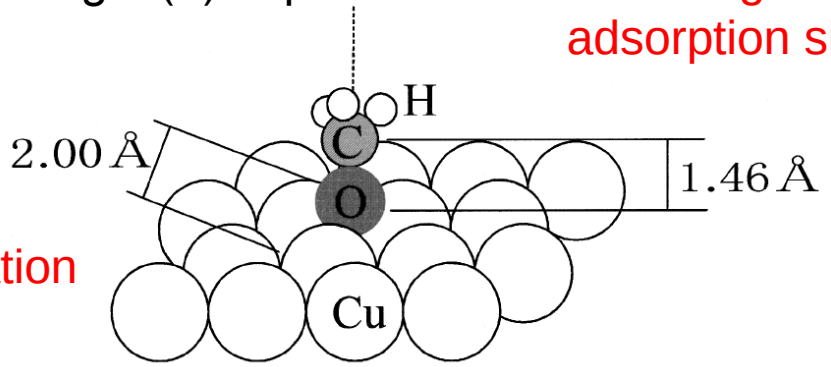

Determination of Atomic Structure

S K-edge EXAFS

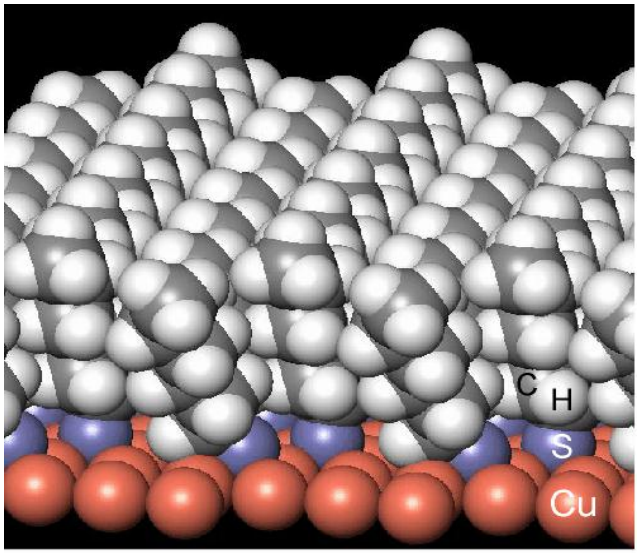

$C_6H_{13}S/Cu(100)$

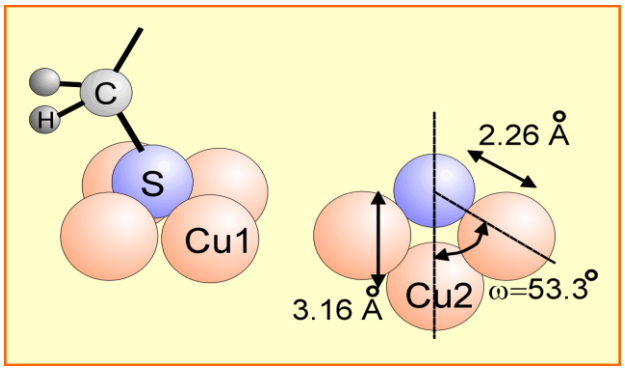

Surface-EXAFS

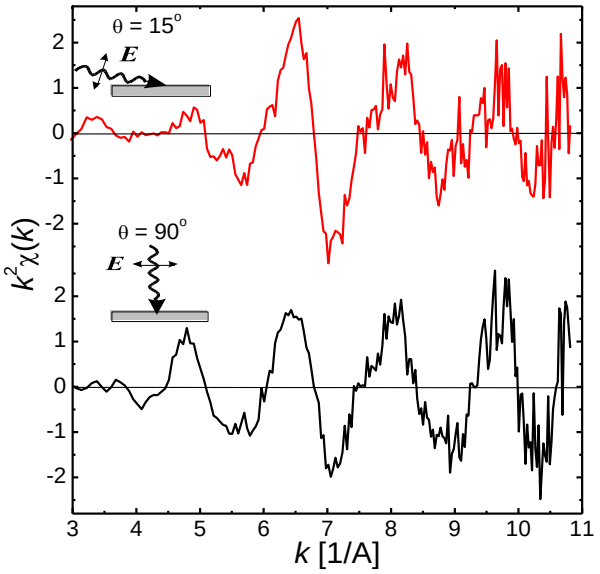

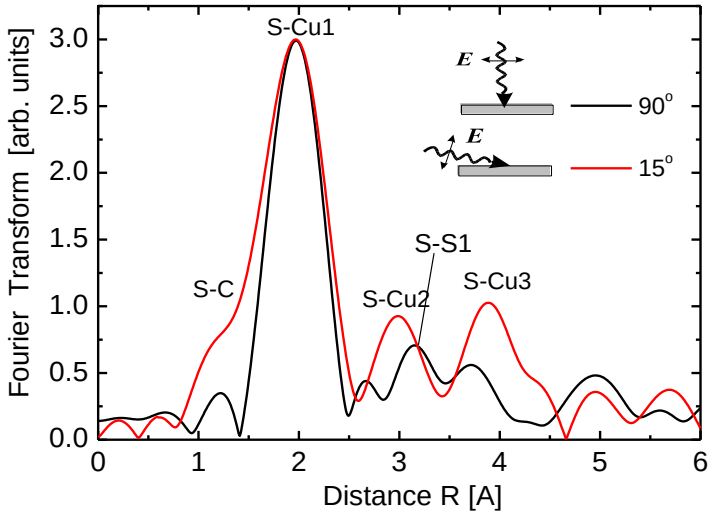

Magnetic structures studied by XMCD

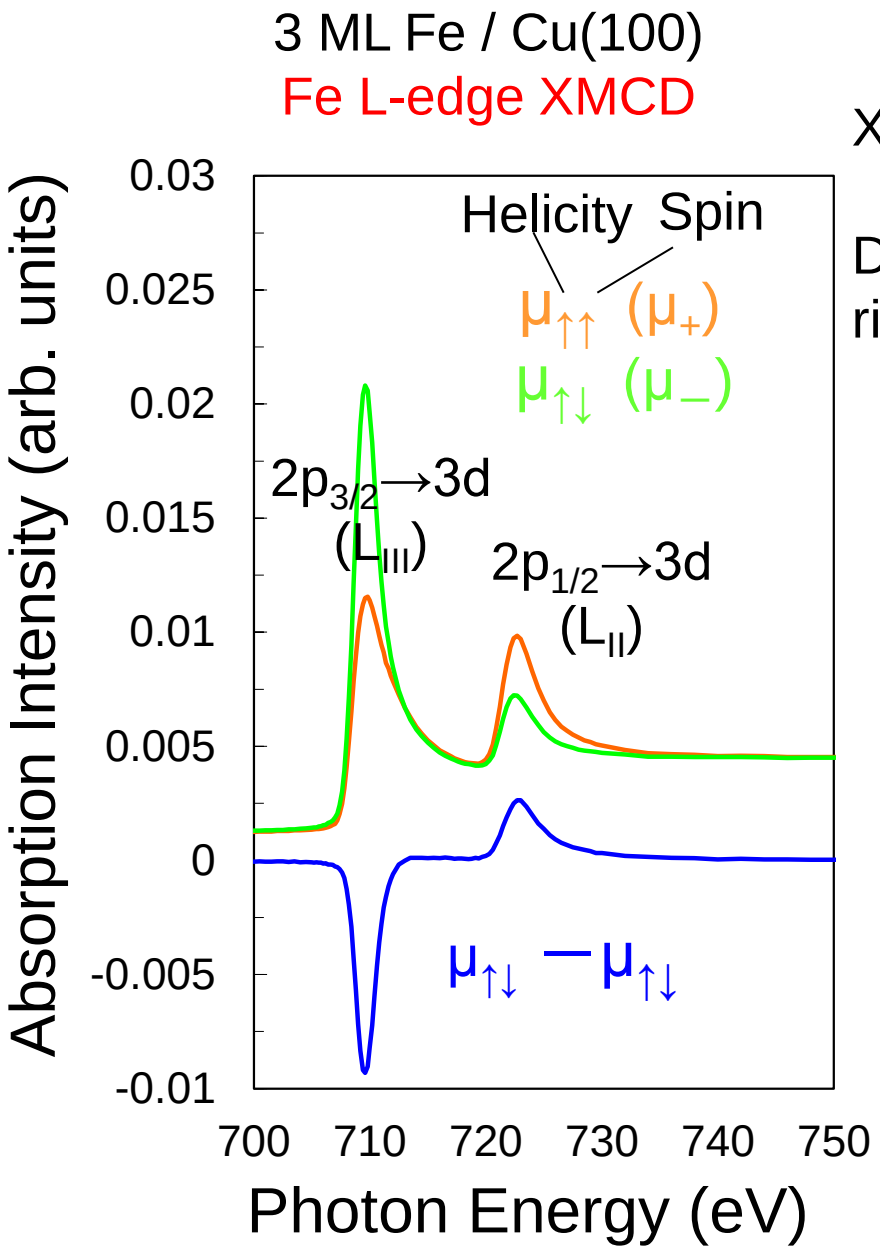

X-ray Magnetic Circular Dichroism (XMCD)

Difference in absorption intensities between right- and left-hand circular polarizations

1. Element Selectivity
   <- resonant absorption (2p->3d…)
2. Determination of Spin and Orbital magnetic moments
   ← Sum rules
3. High Sensitivity

Principle of XMCD

No 3d orbital moment

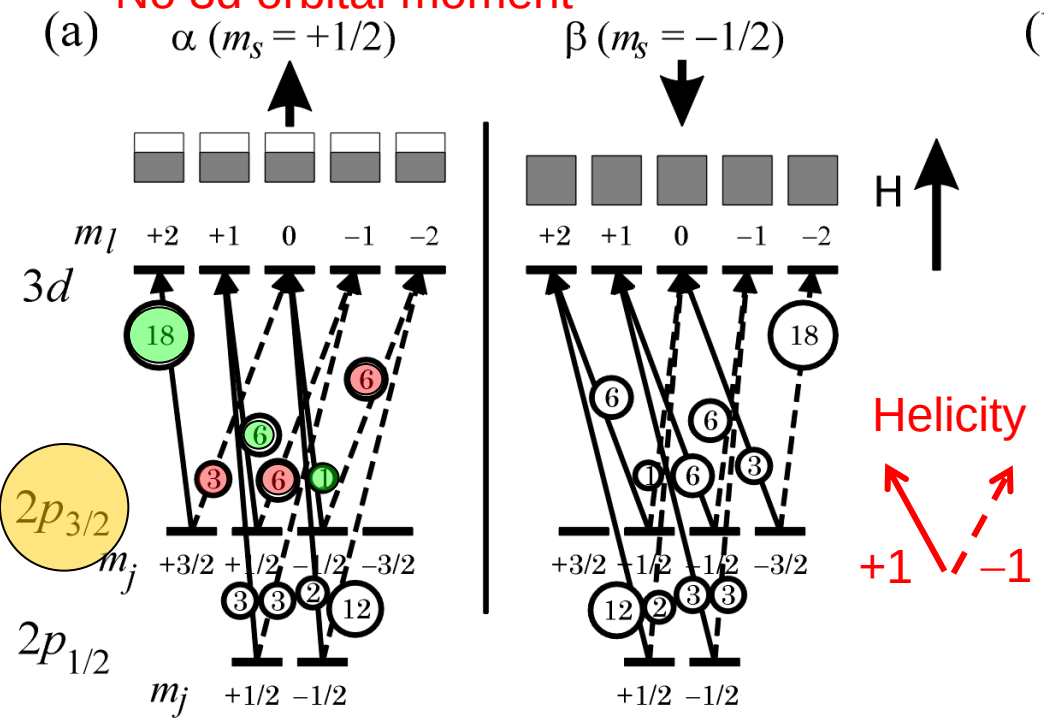

Finite 3d orbital moment

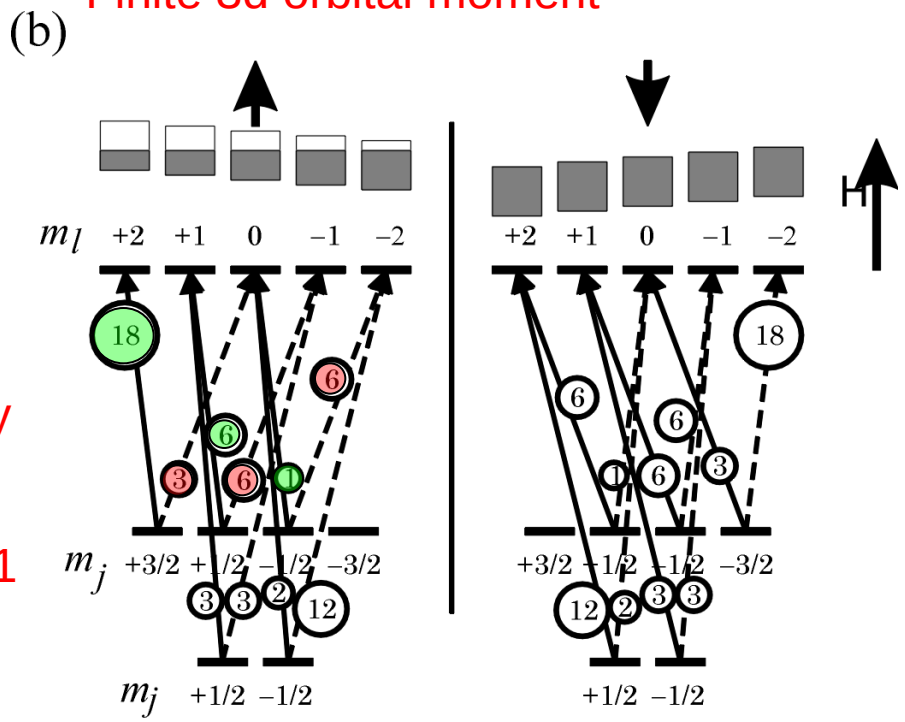

$\mu_{\uparrow\uparrow}$= 3+6+6=15

$\mu_{\uparrow\downarrow}$= 18+6+1=25

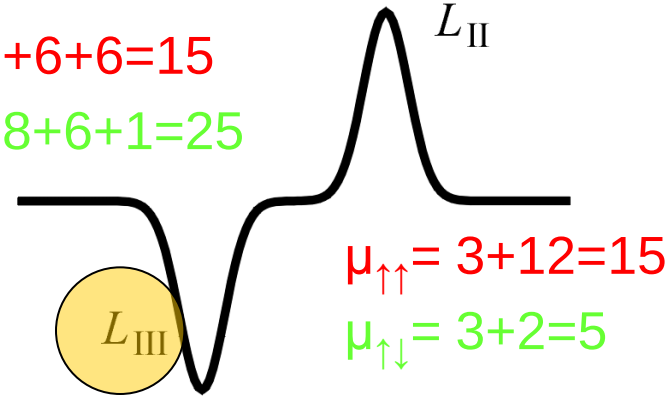

$\mu_{\uparrow\uparrow}$= 3+12=15

$\mu_{\uparrow\downarrow}$= 3+2=5

$\mu_{\uparrow\uparrow}$< 15

$\mu_{\uparrow\downarrow}$> 25

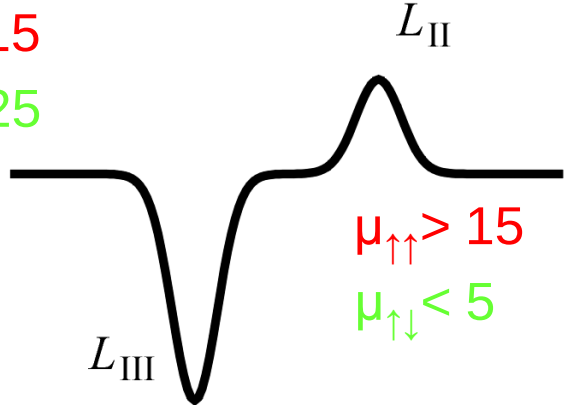

$\mu_{\uparrow\uparrow}$> 15

$\mu_{\uparrow\downarrow}$< 5

XMCD Sum Rules

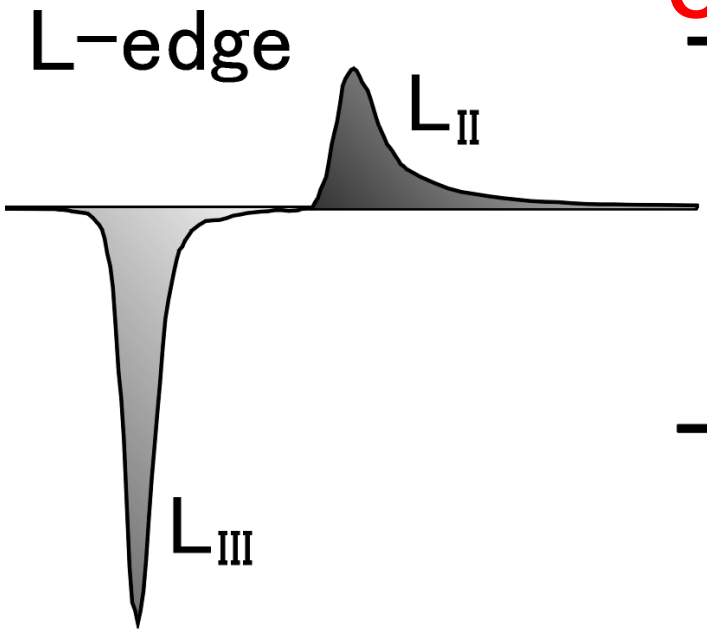

Orbital moment m_l

$$\frac{\int L_{III}(\mu_+ - \mu_-) + \int L_{II}(\mu_+ - \mu_-)}{}$$

$$< 0 \rightarrow \quad m_l > 0$$

Spin moment m_s

$$\frac{\int L_{III}(\mu_+ - \mu_-) - 2\int L_{II}(\mu_+ - \mu_-)}{}$$

$$< 0 \rightarrow \quad m_s > 0$$

B.T. Thole et al., PRL **68**, 1943 (1992).
P. Carra et al., PRL **70**, 694 (1993).

Magnetism of Thin Films Studied by XMCD

Co *L*-edge XMCD spectra

P. Gambardella, Nature **416**, 301 (2002)

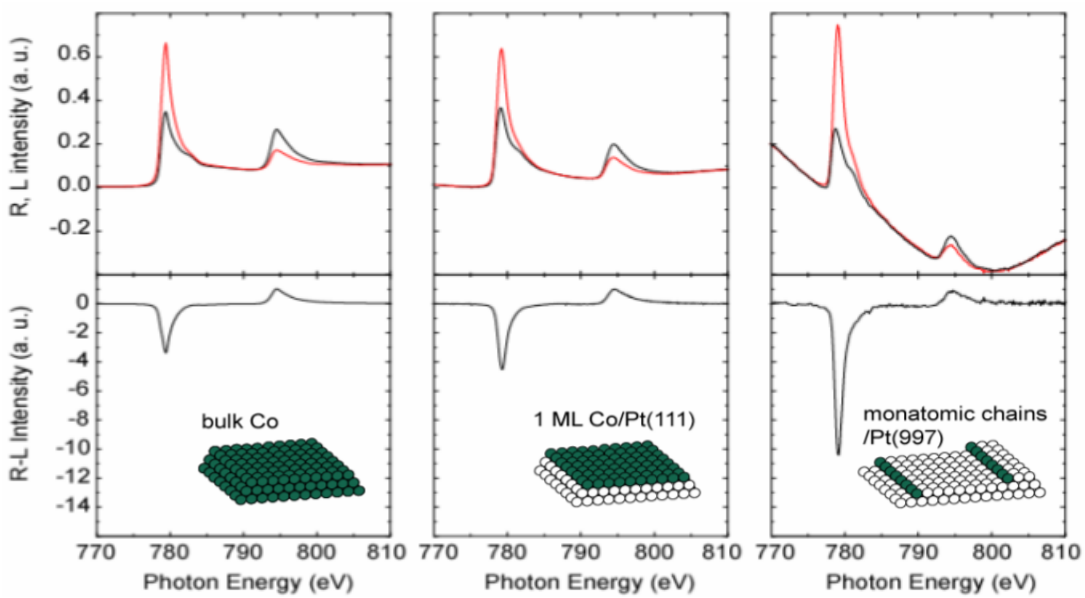

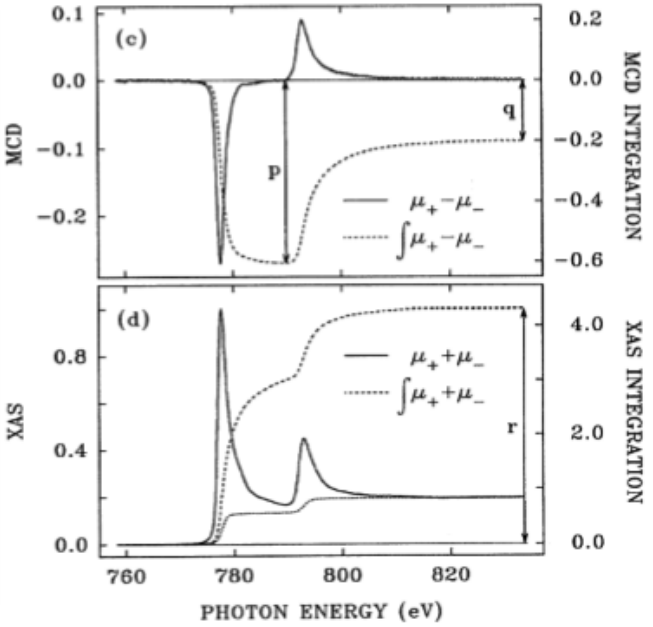

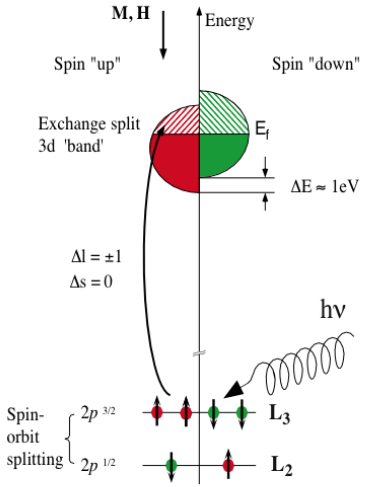

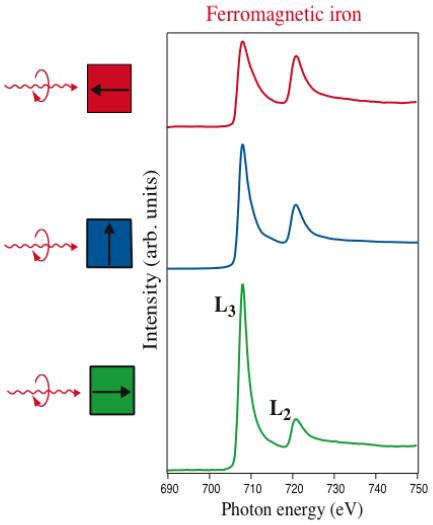

XMCD sum rules

$$m_{orb} = \frac{4q}{3r}(10 - n_{3d})$$

$$m_s = \frac{6p - 4q}{r}(10 - n_{3d})$$

$$\frac{m_{orb}}{m_s} = \frac{2q}{9p - 6q}$$

$$r = \int_{L_{2,3}} (\mu_+ + \mu_-) d\omega$$

$$p = \int_{L_3} (\mu_+ - \mu_-) d\omega$$

$$q = \int_{L_{2,3}} (\mu_+ - \mu_-) d\omega$$

C.T. Chen et al., PRL **75**, 152 (1995)

Utilization of Element Selectivity of XMCD

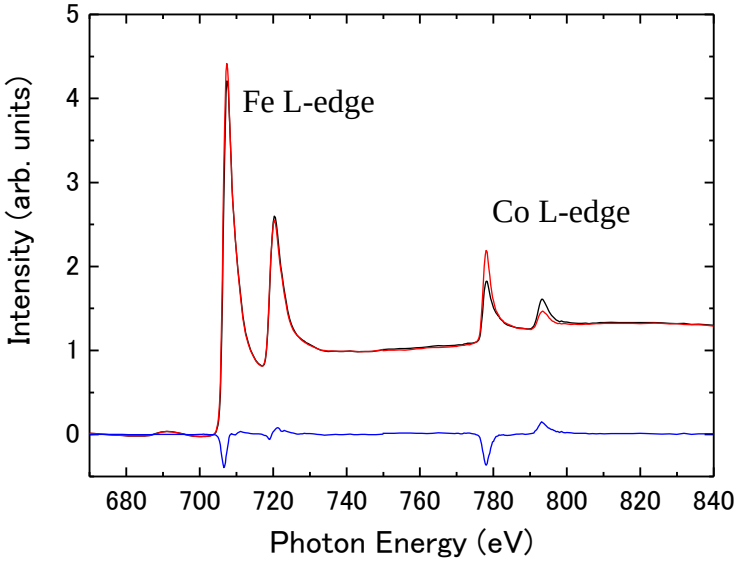

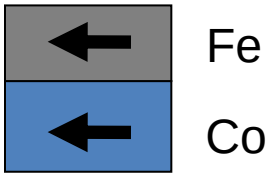

Magnetic-field dependence of XMCD at Fe and Co L edges

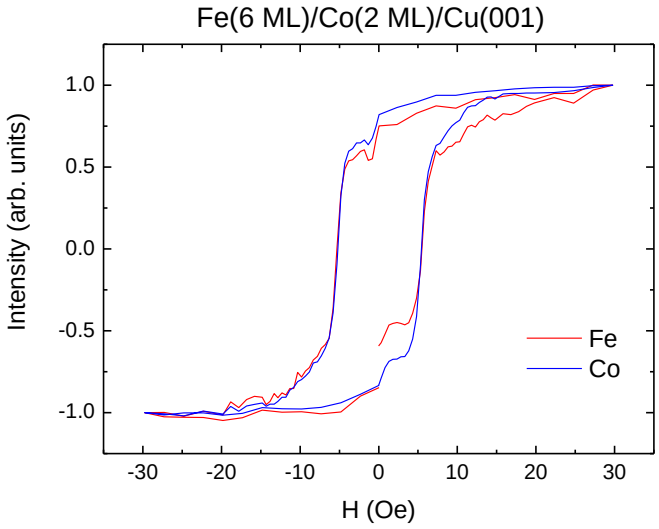

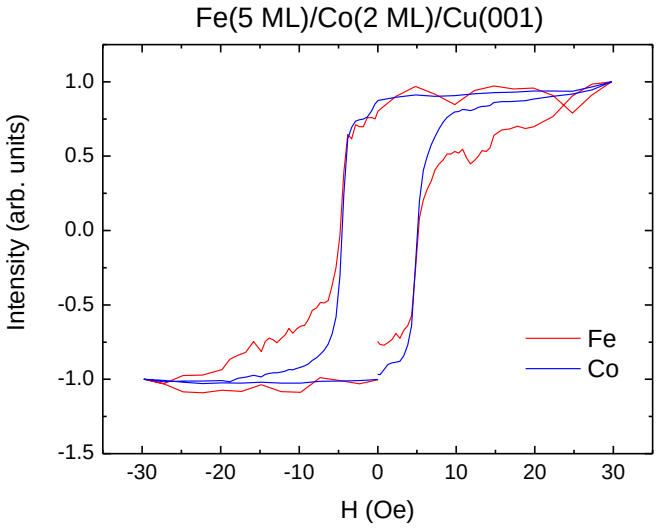

Angle Dependence of XMCD
(1) weak magnetic field or remanent measurements

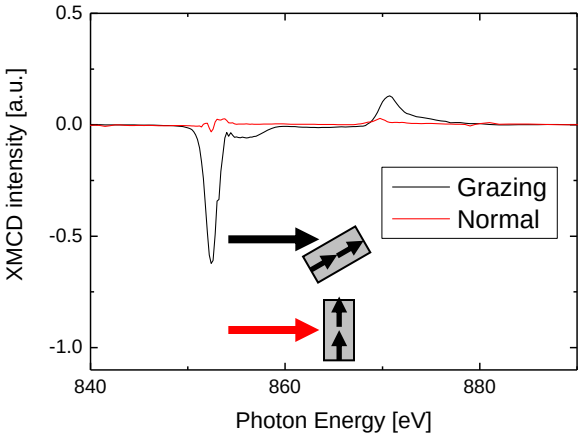

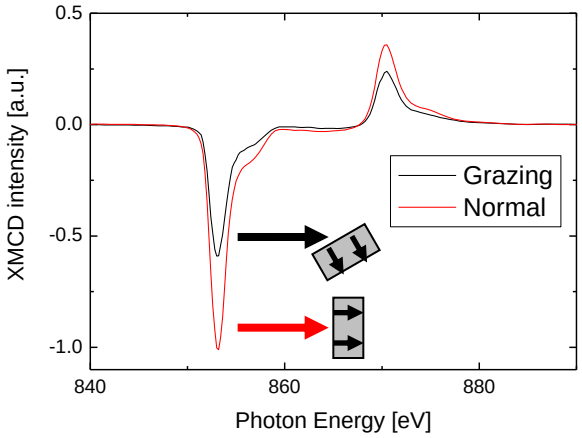

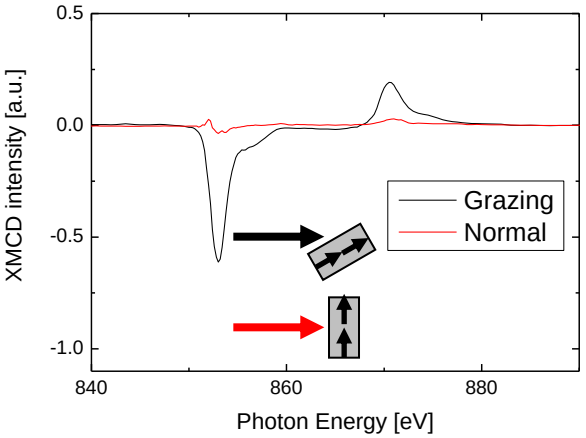

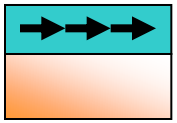

Ni (7.5 ML)
Cu(100)

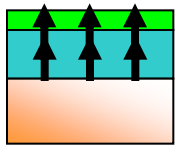

Fe (0.7 ML)
Ni (7.5 ML)
Cu(100)

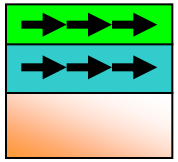

Fe (4 ML)
Ni (7.5 ML)
Cu(100)

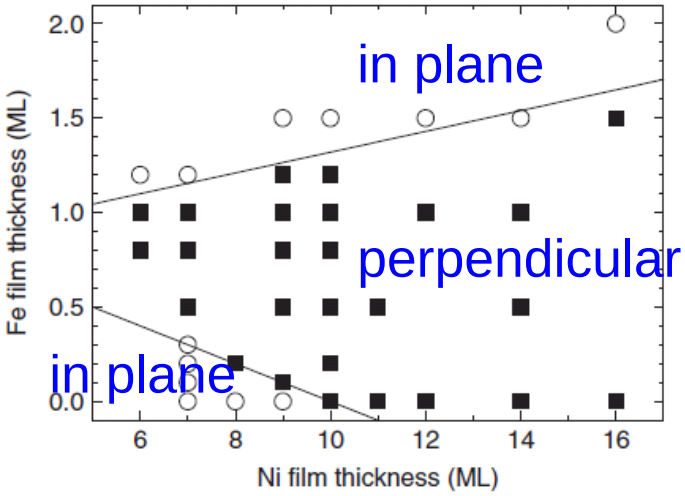

XMCD reflects magnetic component which is parallel to X-ray beam.
-> determination of easy axis of magnetization

Information on orbital moment
-> estimation of magnetic anisotropy

Abe et al., J. Magn. Magn. Mater. 206 (2006) 86.

Angle Dependence of XMCD
(2) High magnetic field measurements

XMCD (X-ray Magnetic Circular Dichroism)

Element selectivity

Quantitative determination of spin & orbital magnetic moments by using the sum rules

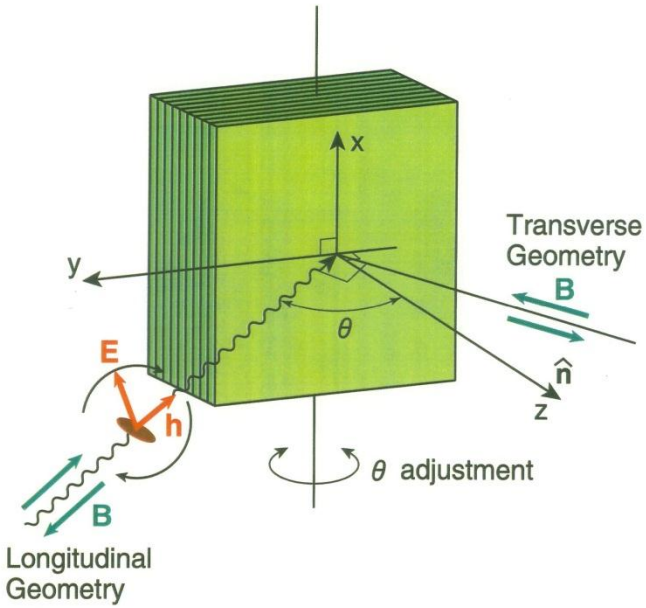

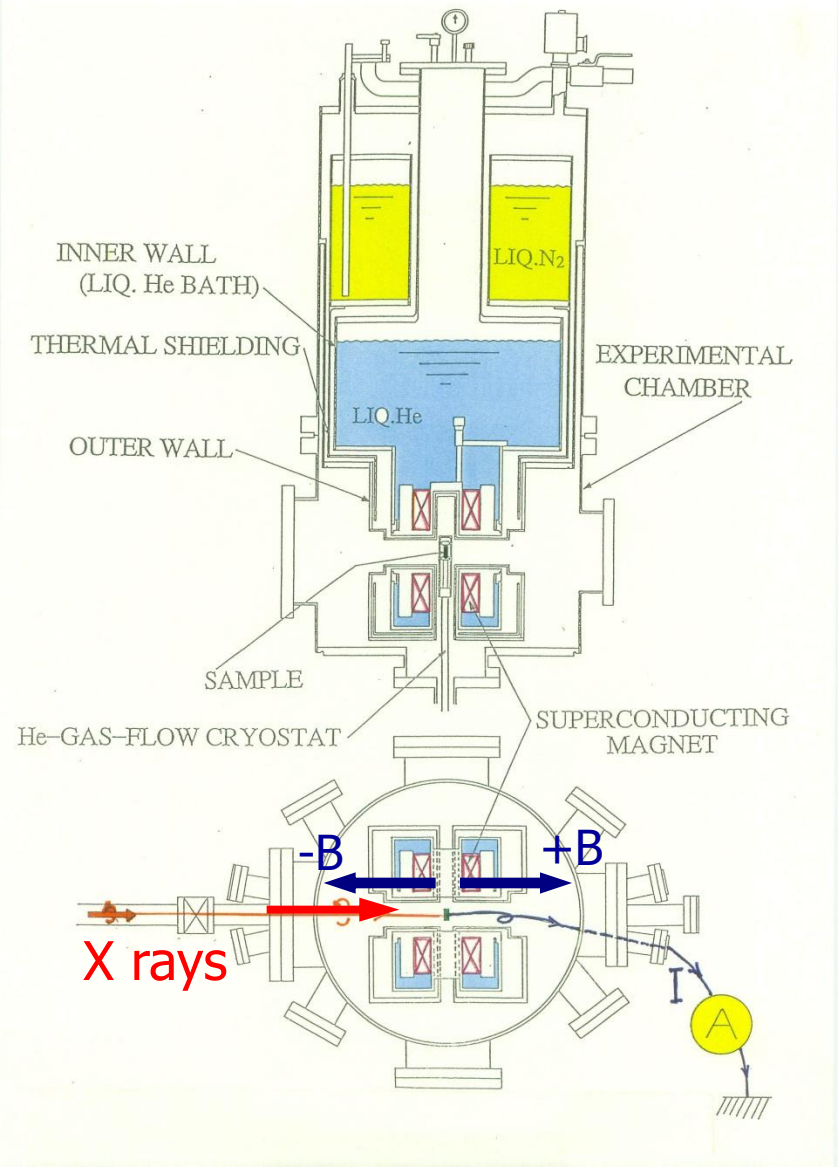

Angle-dependent XMCD

⇒ **Magnetic anisotropy**

Separation of m_s from m_T

T. Koide et al., Rev. Sci. Instrum. **63**, 1462 (1992).

Angle-dependent XMCD Sum Rules

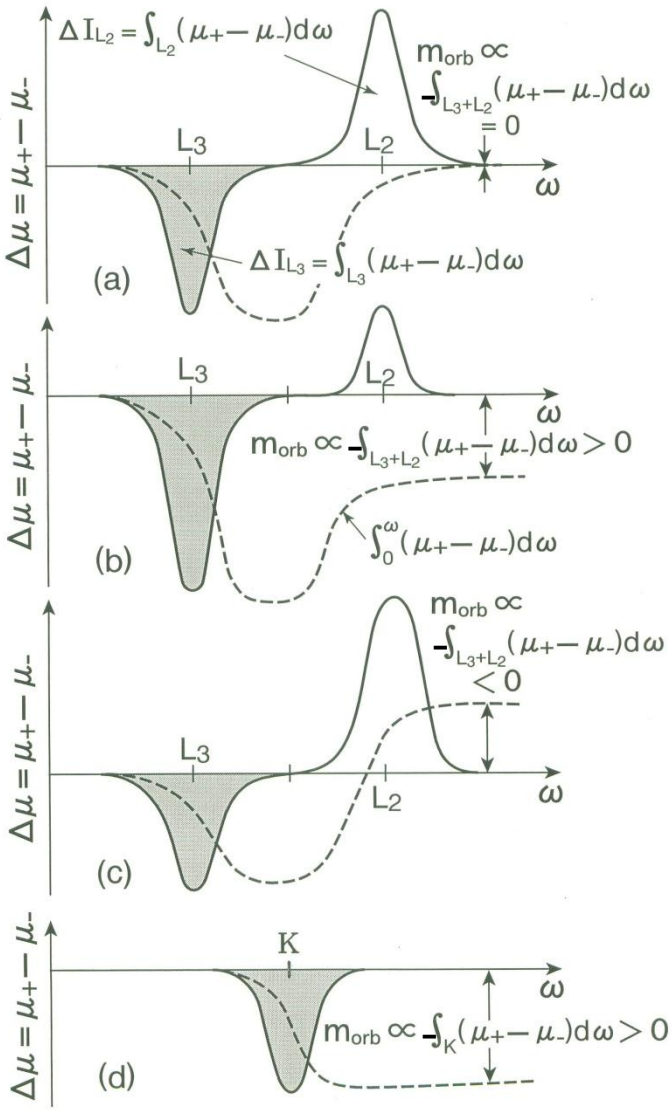

Orbital sum rule

$$\frac{[\Delta I_{L_3} + \Delta I_{L_2}]^{\theta}}{I_{L_3} + I_{L_2}} = -\frac{3 \cdot m_l^{\theta}}{4 n_h \cdot \mu_B}$$

Spin sum rule

$$\frac{[\Delta I_{L_3} - 2 \cdot \Delta I_{L_2}]^{\theta}}{I_{L_3} + I_{L_2}} = -\frac{(m_s + 7 \cdot m_T^{\theta})}{2 n_h \cdot \mu_B}$$

B.T. Thole et al., PRL **68**, 1943 (1992).
P. Carra et al., PRL **70**, 694 (1993).

$$m_l^{\theta} = m_l^{\perp} \cos^2\theta + m_l^{//} \sin^2\theta$$
$$m_T^{\theta} = m_T^{\perp} \cos^2\theta + m_T^{//} \sin^2\theta$$

Investigation of Interface Magnetism

T. Koide et al., Phys. Rev. Lett. 87, 257201 (2001)

Au/Co(2 ML)/Au(111)

Self-assembled Co islands due to a reconstruction of Au surface

All Co atoms are regarded to "interface" because of 2 ML thickness

⇒ **Direct observation of interface magnetism**

Angle-dependent XMCD

⇒ **Direct determination of** m_s, $m_l^{//}$, $m_l^{\perp}$, $m_T^{//}$, $m_T^{\perp}$

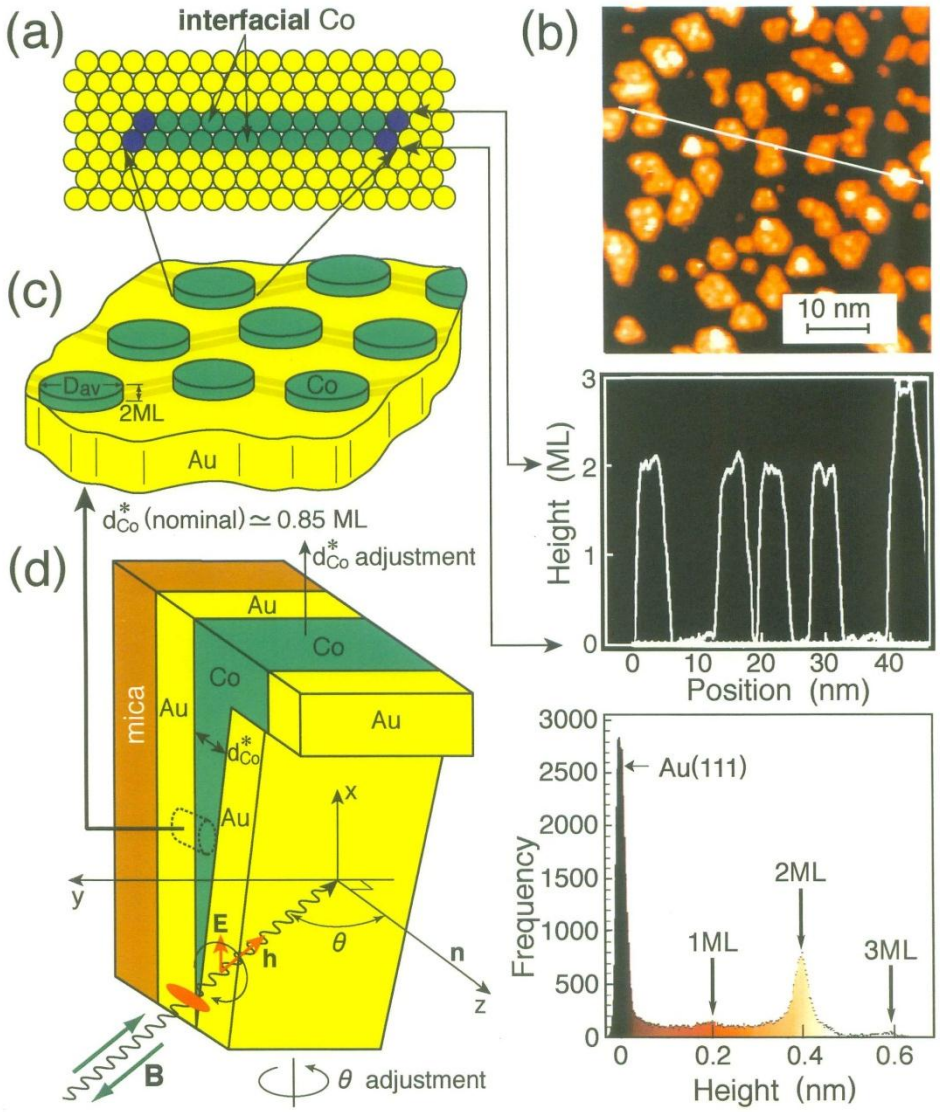

Angle-dependent XMCD Measurements

T. Koide et al., Phys. Rev. Lett. 87, 257201 (2001)

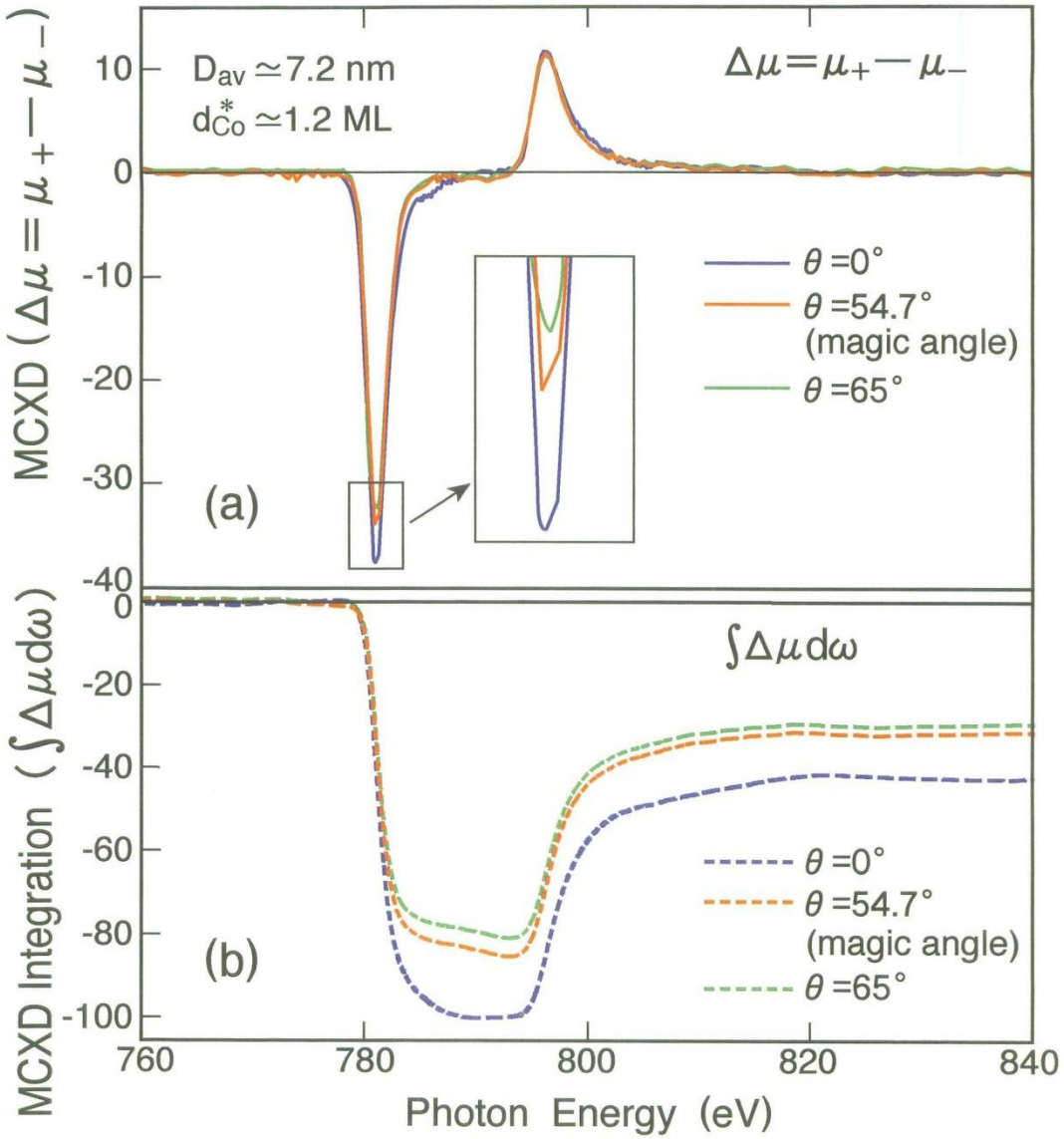

PF BL-11A

Angle dependence in XMCD
← Anisotropy in m_l, m_T

$$m_j^{\theta} = m_j^{\perp}\cos^2\theta + m_j^{//}\sin^2\theta$$
(j = l or T)

$$m_T^{\perp} + 2\, m_T^{//} = 0$$

⇒ Determination of all moments including their anisotropy

Determined Magnetic Moments

T. Koide et al., Phys. Rev. Lett. 87, 257201 (2001)

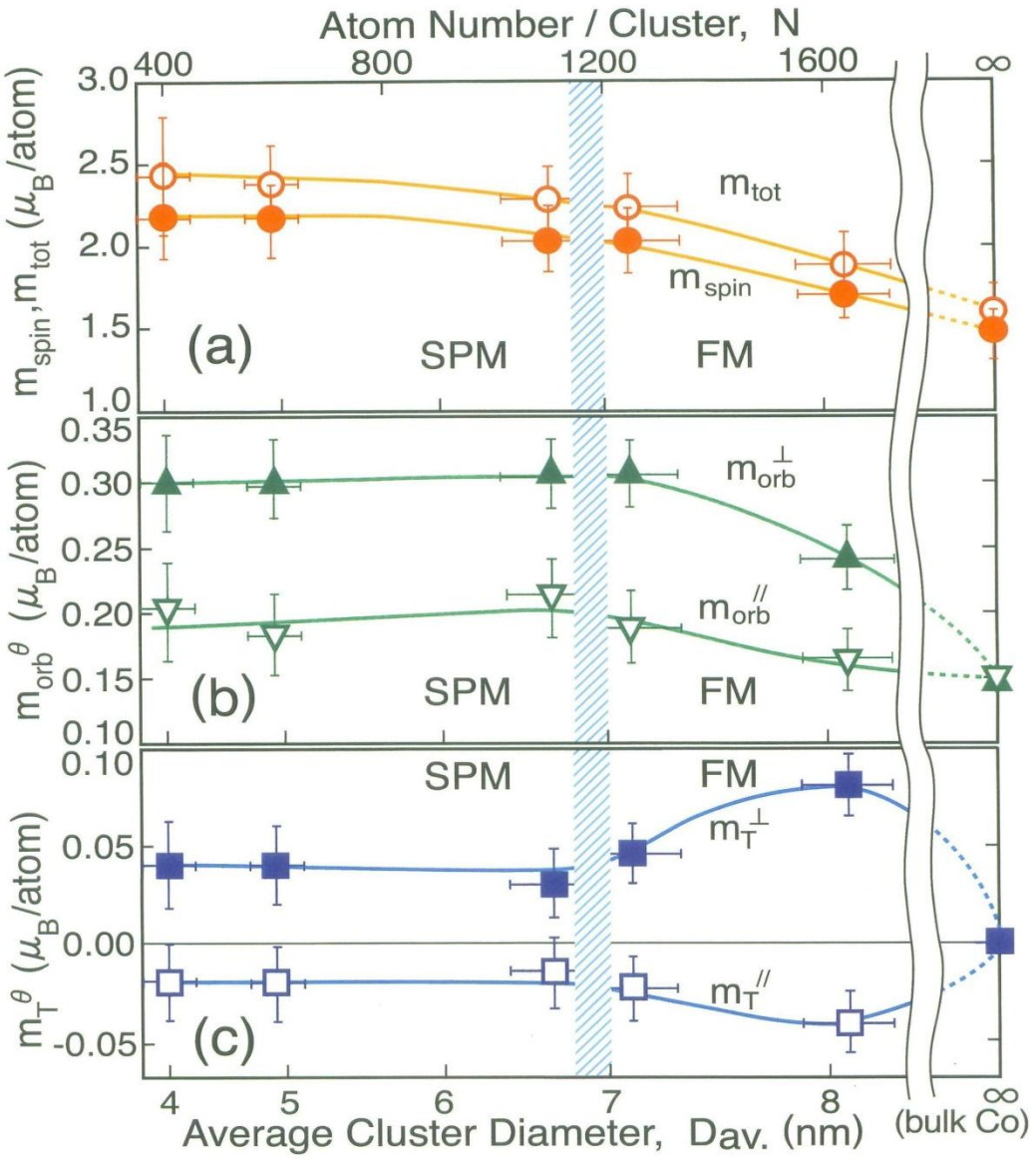

Cluster-size dependent phase transition

1. Advantages and Disadvantages of

   Soft X-ray Absorption Spectroscopy (SXAS)

2. SXAS studies on Surface and Thin films

3. Novel SXAS Techniques

   3-1. Depth-resolved XAS

   3-2. Wavelength-dispersive XAS

Introduction: Exploring Magnetic Depth Profile

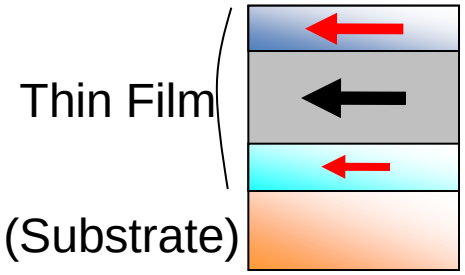

Surface and interface show different magnetism from inner layers

Surface and Interface sometimes affect magnetism of whole film

Surface effect: Gas adsorption

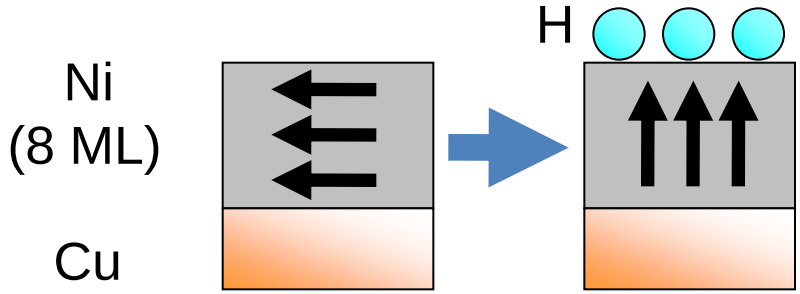

Vollmer, et al., Phys. Rev. B 60 (1999) 6277.

Adsorption-induced change in magnetic easy axis

⇒ What happens at surface?

Interface effect: TMR

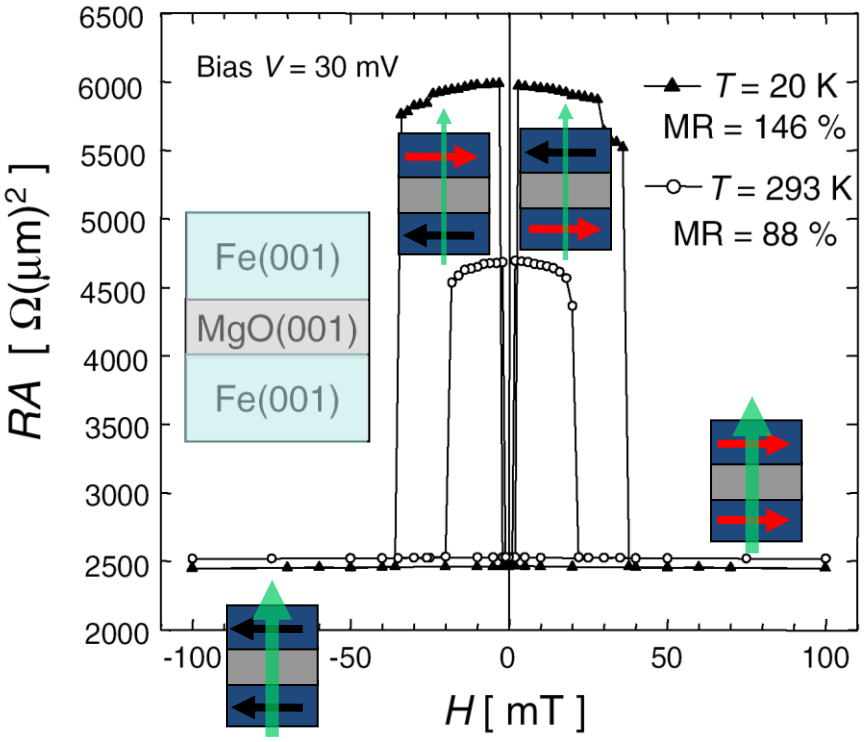

Fig. 3. Magnetoresistance curves for Fe(001)/MgO(001)(20 Å)/Fe(001) MTJ at $T = 293$ and 20 K. The MR ratios were 88% and 146%, respectively.

Yuasa, et al., Jpn. J. Appl. Phys. 43 (2004) L588.

Chemical and magnetic states at interface affect MR ratio

Co/Cu(100) - Surface & interface orbital moment -

Tischer et al., PRL 75 (1995) 1602.

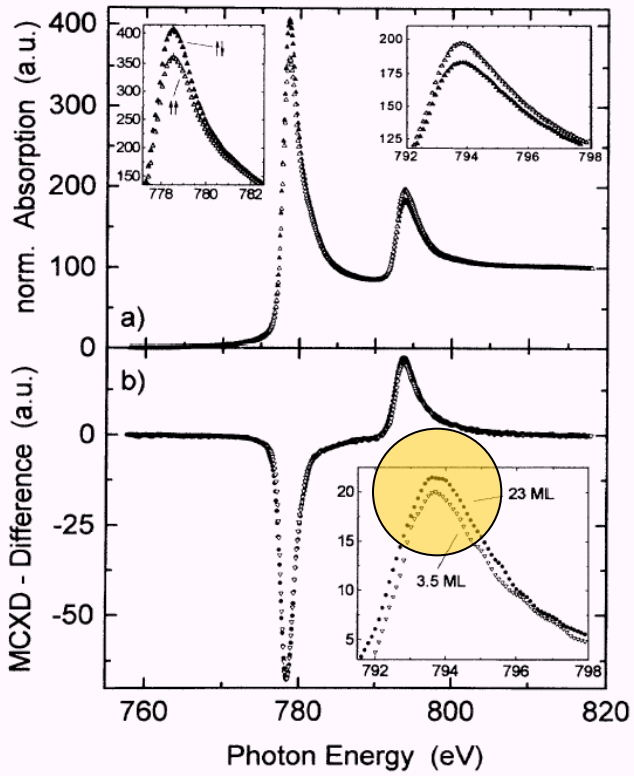

FIG. 2. (a) The normalized absorption spectrum for 3.5 ML Co/Cu(100). Open triangles indicate the photon spin parallel to the remanent magnetization, full triangles antiparallel. (b) MCXD difference for the 3.5 ML film (triangles) and a thick 23 ML film (circles). Both are normalized to the same L_3 intensity to demonstrate that the dichroic response around the L_2 edge is relatively smaller for the thin film.

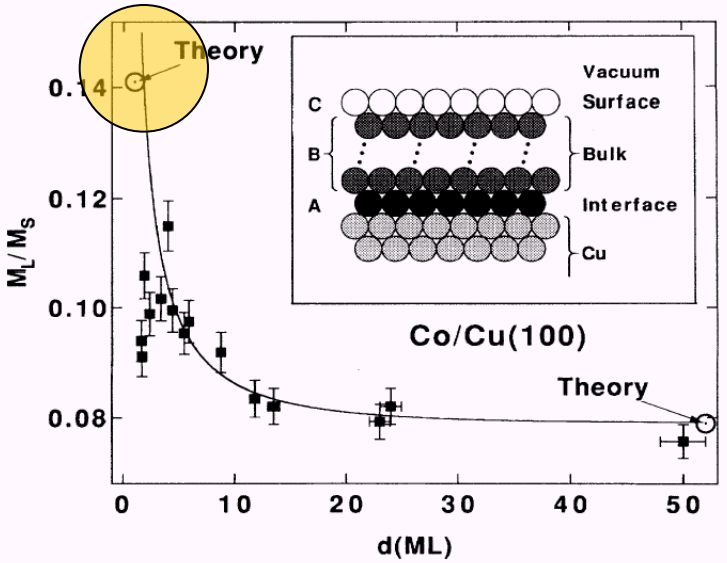

FIG. 3. The ratio of orbital versus spin moment M_L/M_S as a function of film thickness d. The open circles give the theory taken from Table I. The full squares show the experiment. The solid line is a fit using Eq. (1) with the parameters given in the last row of Table I. Note that the fit was performed only for $d \geq 3$ ML, corresponding to well-defined, epitaxial growth. The surface, interface, and bulk contributions used in Eq. (1) are schematically shown in the inset.

[Pt/Co(111)] multilayer - Interface orbital moment -

Nakajima et al., PRL 81 (1998) 5231.

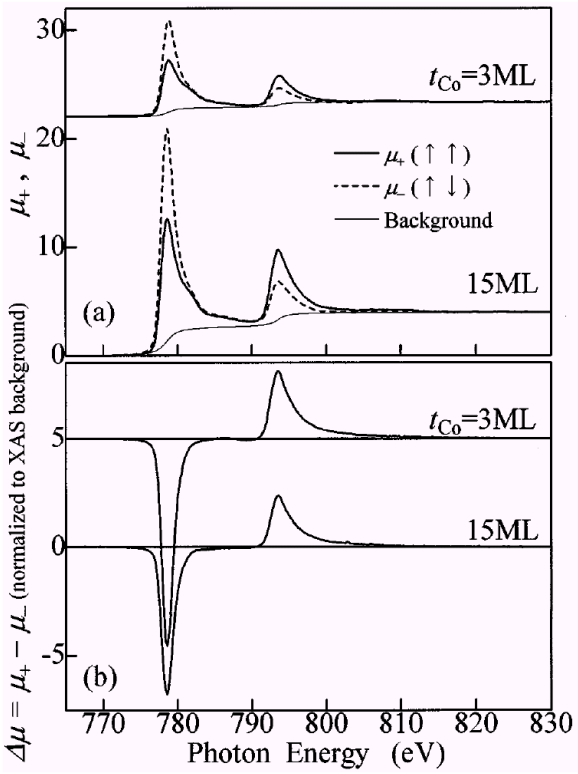

FIG. 2. (a) Polarization-dependent Co $L_{2,3}$ XAS spectra of Co(t_{Co})/Pt(7.5 ML) multilayers for t_{Co} = 3 and 15 ML. Correction for P_C was made. The thin solid curve denotes the averaged XAS background. (b) Co $L_{2,3}$ MCXD spectra normalized by the edge jump above 820 eV in XAS of (a).

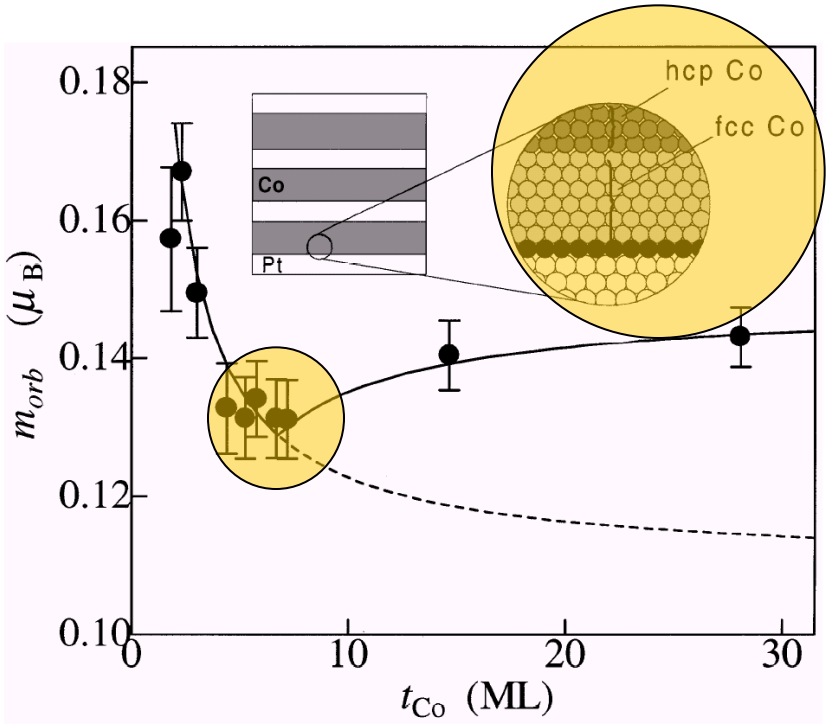

FIG. 3. Orbital magnetic moment of Co perpendicular to the film plane as determined from the MCXD and XAS spectra of Fig. 2 using the MCXD orbital sum rule. The solid curve represents a fit to the data based on the model shown in the inset. The dashed curve denotes an extrapolation for a supposed case of all fcc Co layers.

Conventional Technique for Depth Profiling

SQUID, VSM, MOKE, XMCD…

Gives averaged information over the whole sample.

⇒ also averaged in depth

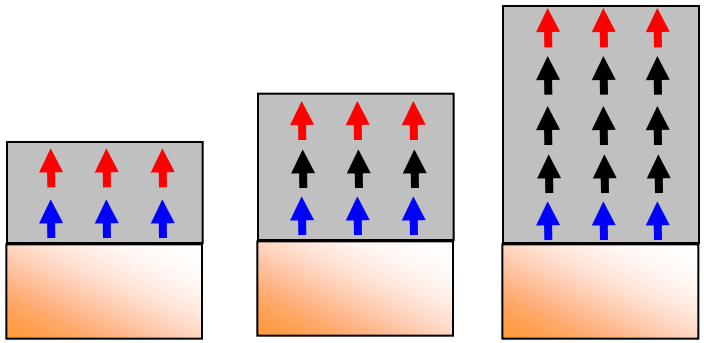

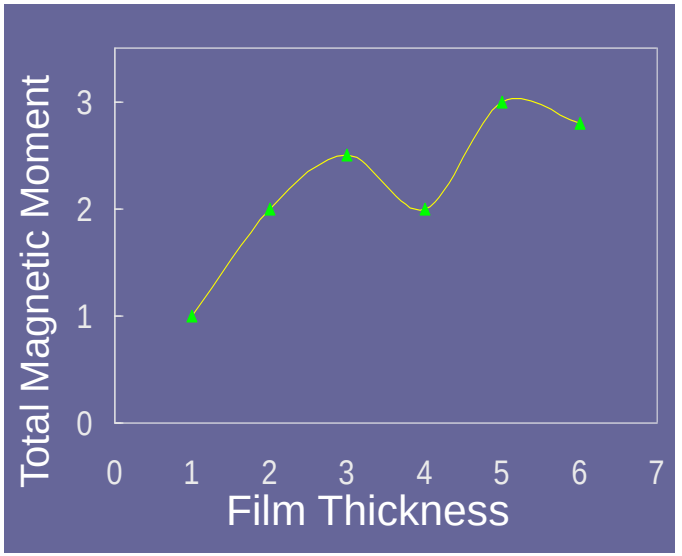

Based on an assumption
that magnetic structure of surface and interface
dose not change upon layer growth

→ Direct technique for depth profiling

XAS Measurement in the Soft X-ray Region

3 ML Fe / Cu(100) Fe L-edge XAS

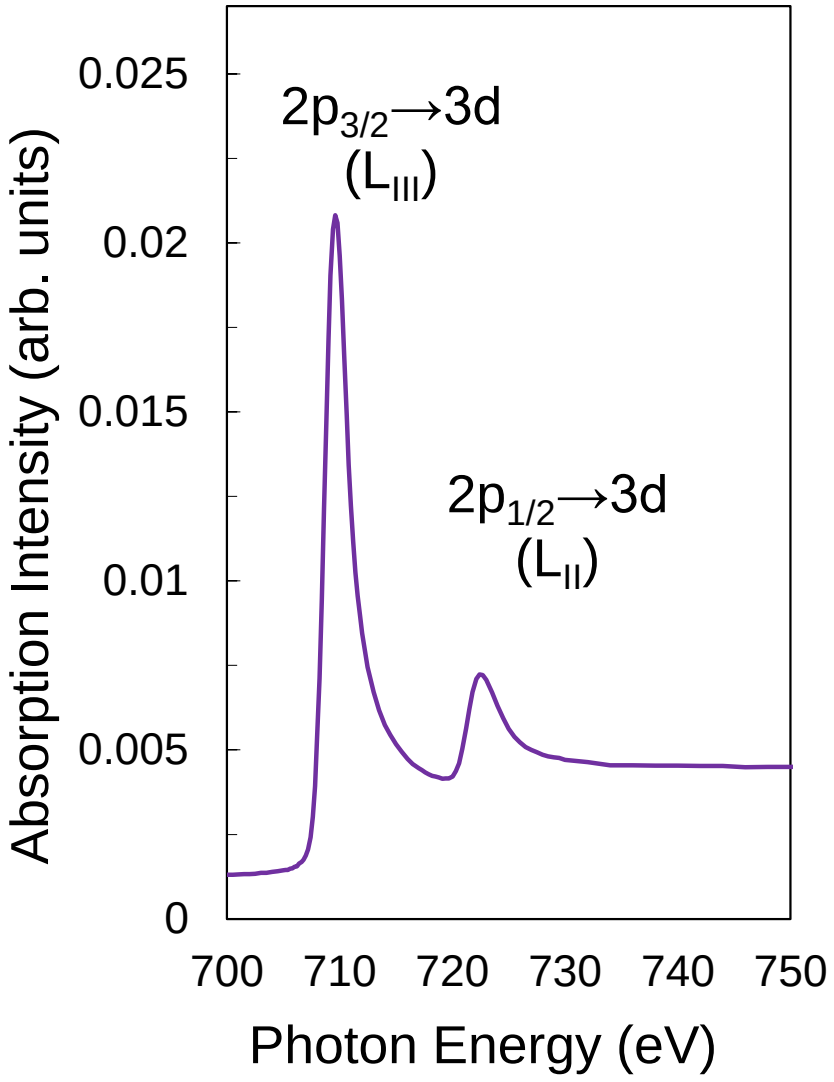

How can we measure

X-ray absorption spectrum ?

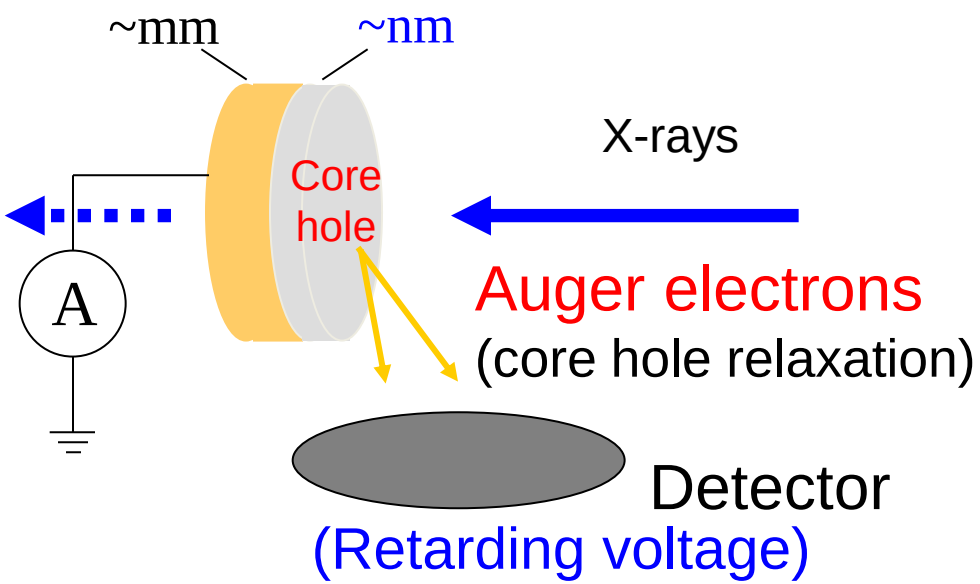

Electron yield XAS

Total electron yield (TEY)

Partial electron yield (PEY)

cf. Fluorescence yield (FY)

Principle of Depth-resolved XAS

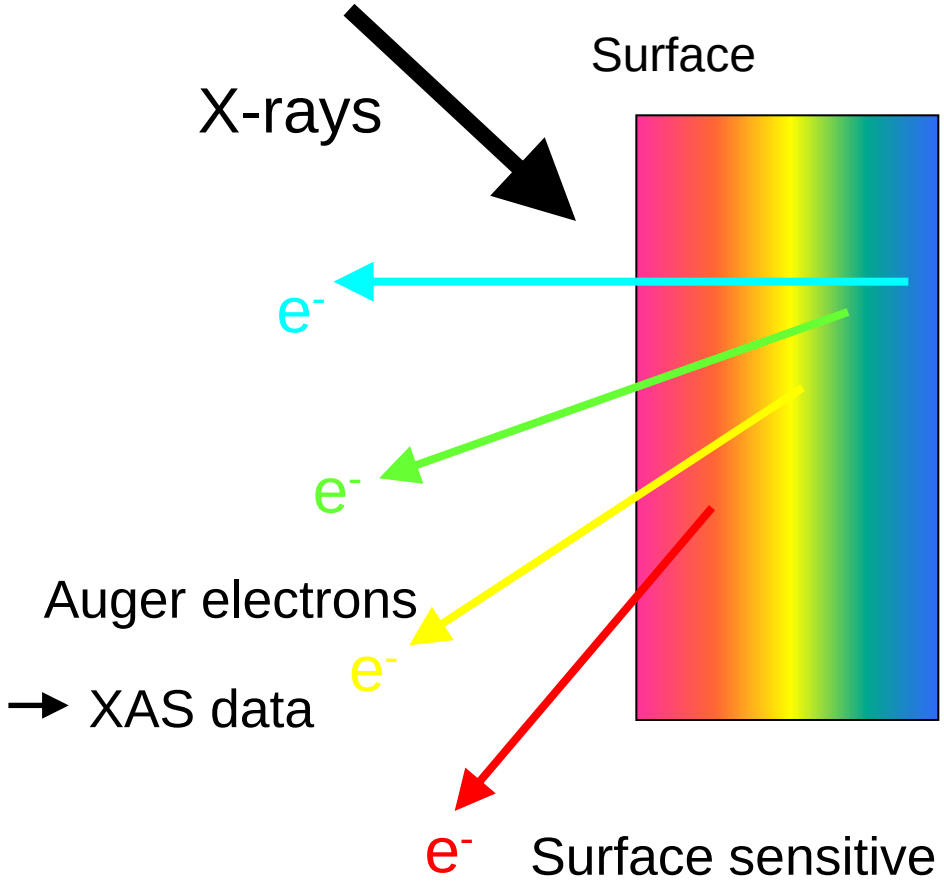

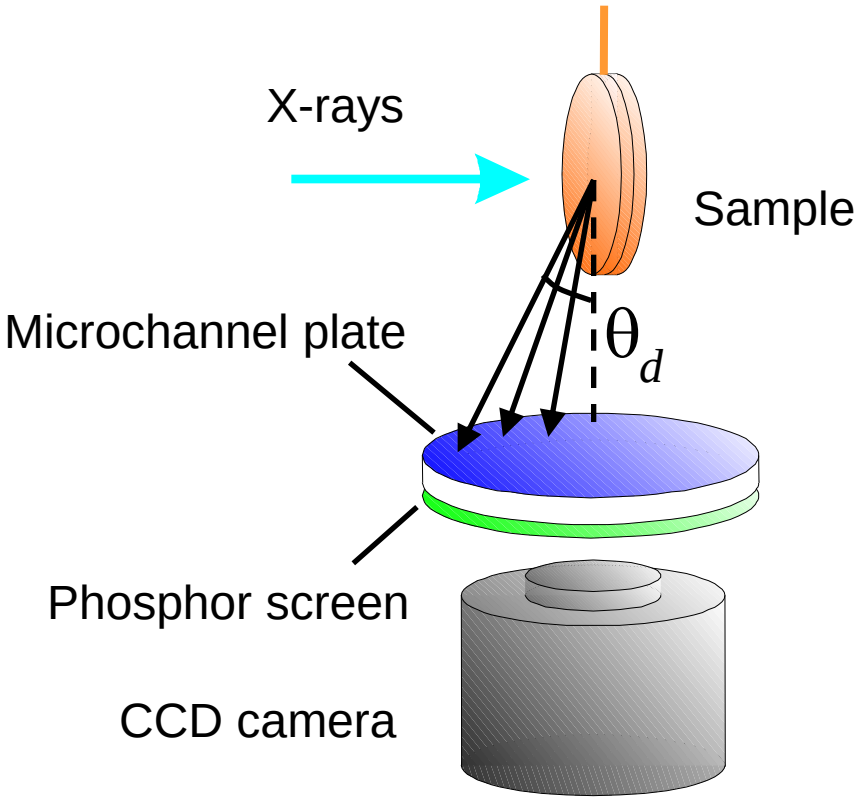

Electron yield XAS measurements at different detection angles

→ A set of XAS data with different probing depths

Probing Depth (effective escape depth) : λ_e

Number of detected electrons emitted at depth z : $I = I_0 \exp(-z/\lambda_e)$

I_0 : Original number of emitted electrons

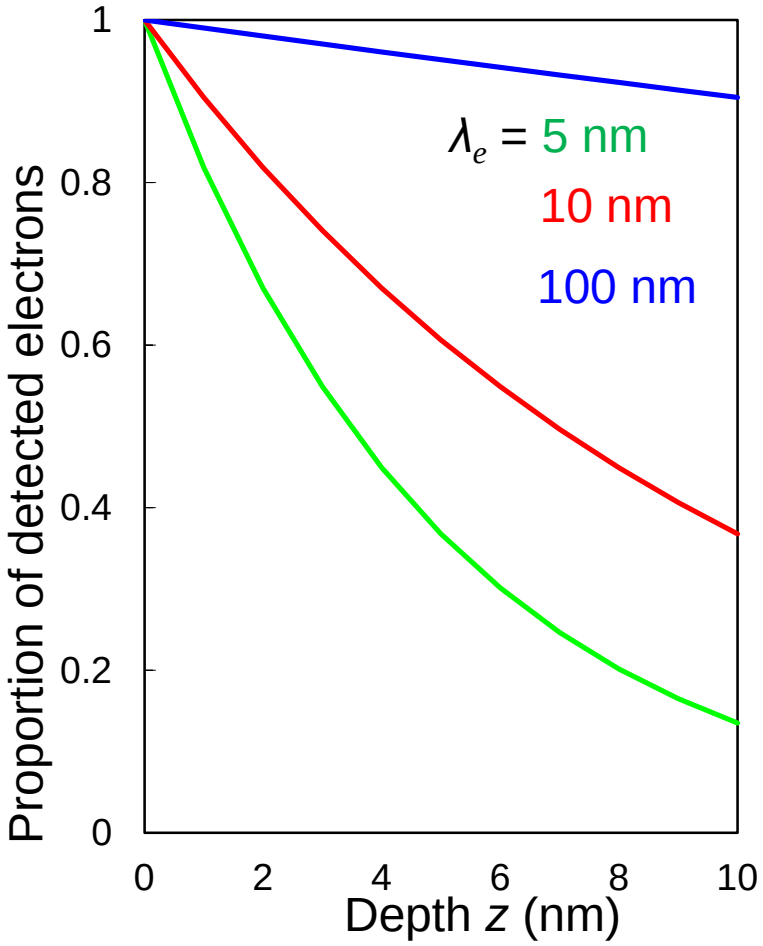

Small λ_e

⇒ Large contribution from surface

XAS:

Averaged information per atom

Depth-resolved XAS :

$\exp(-z/\lambda_e)$-weighted average

Feasibility Study: Depth-resolved XMCD of Fe/Cu(100)

Amemiya et al., APL 84 (2004) 936.

Normal Incidence, 130 K

3 ML Fe

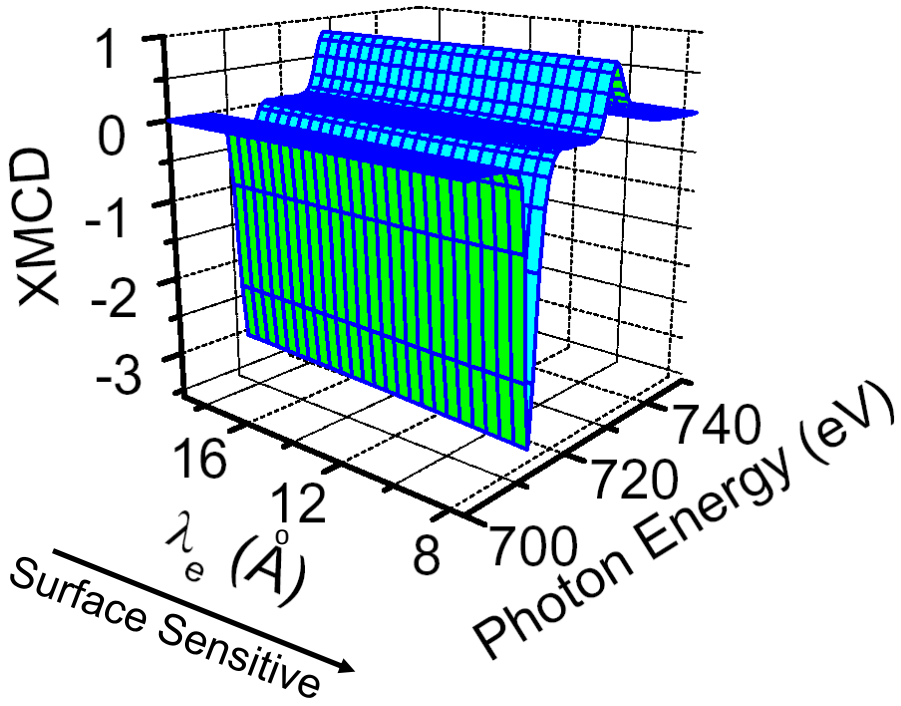

7 ML Fe

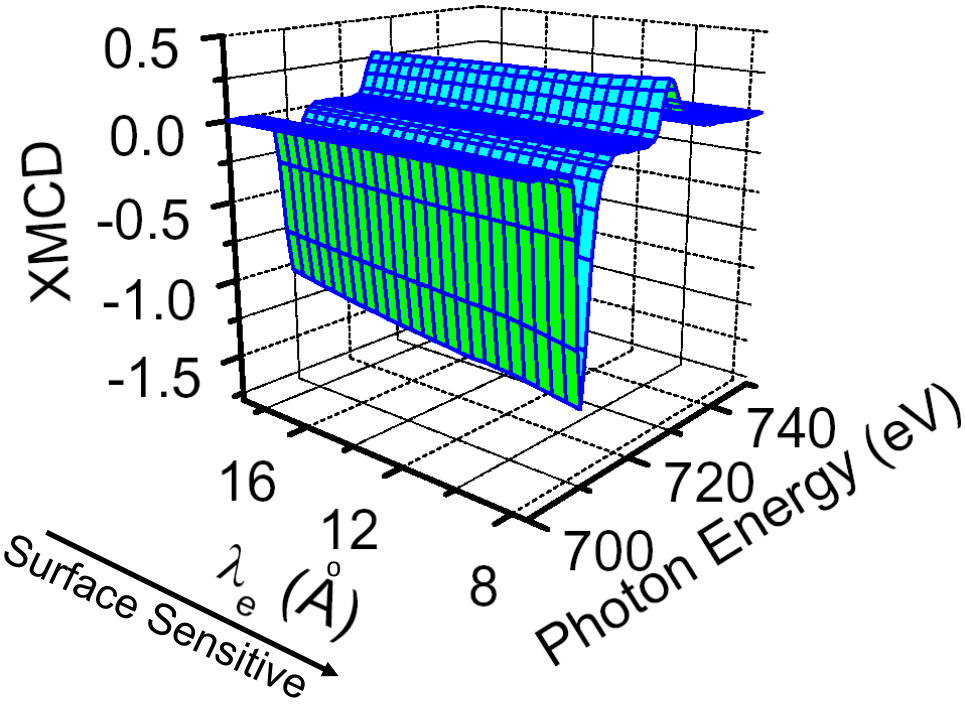

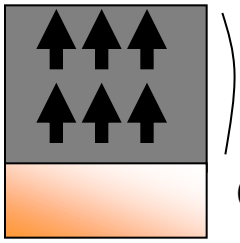

Uniform Magnetization

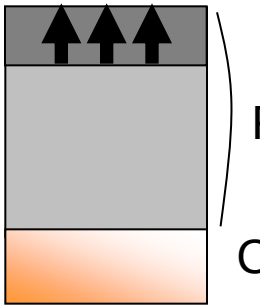

Surface Magnetization

Interpretation of depth-resolved XMCD data

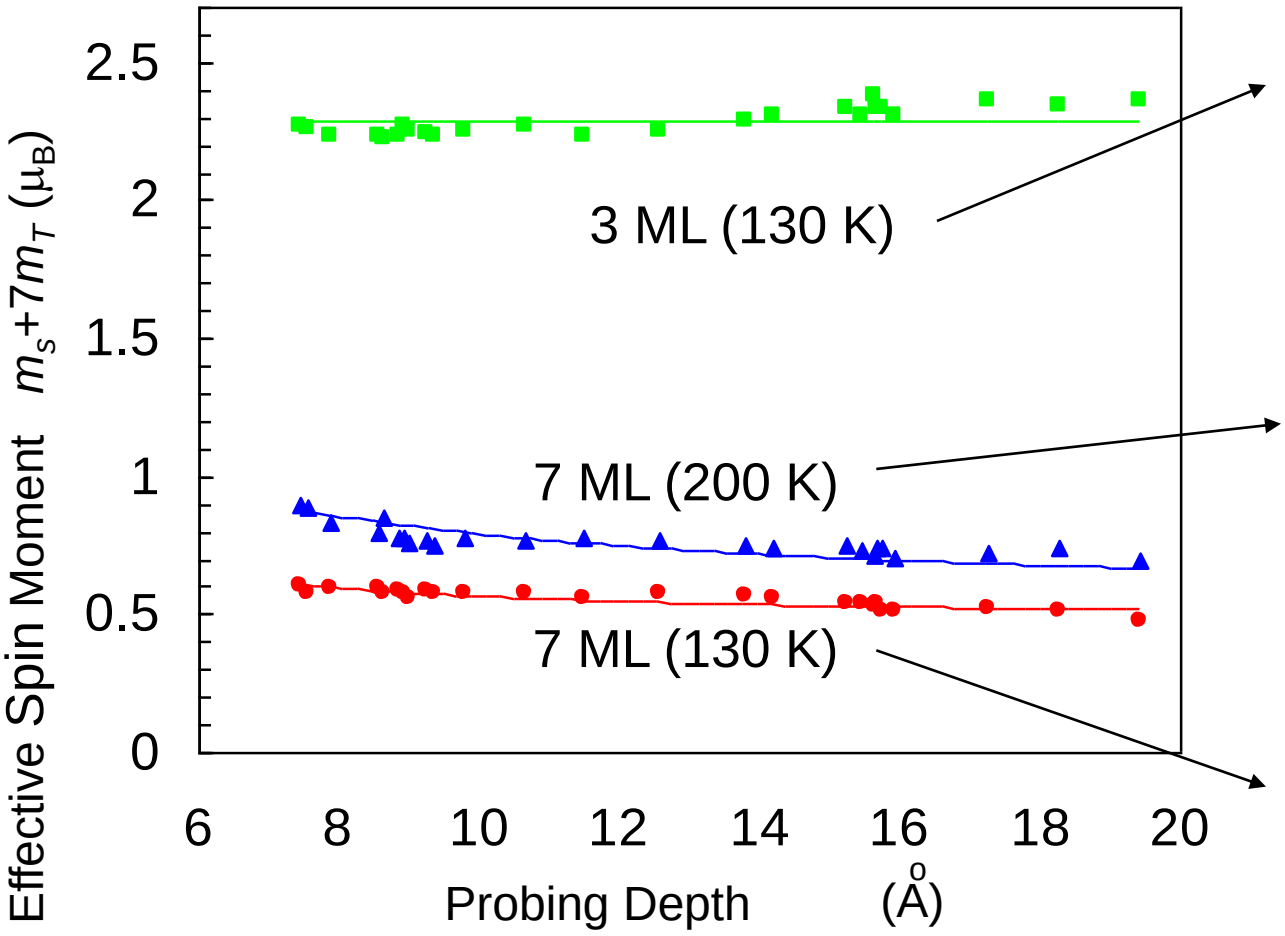

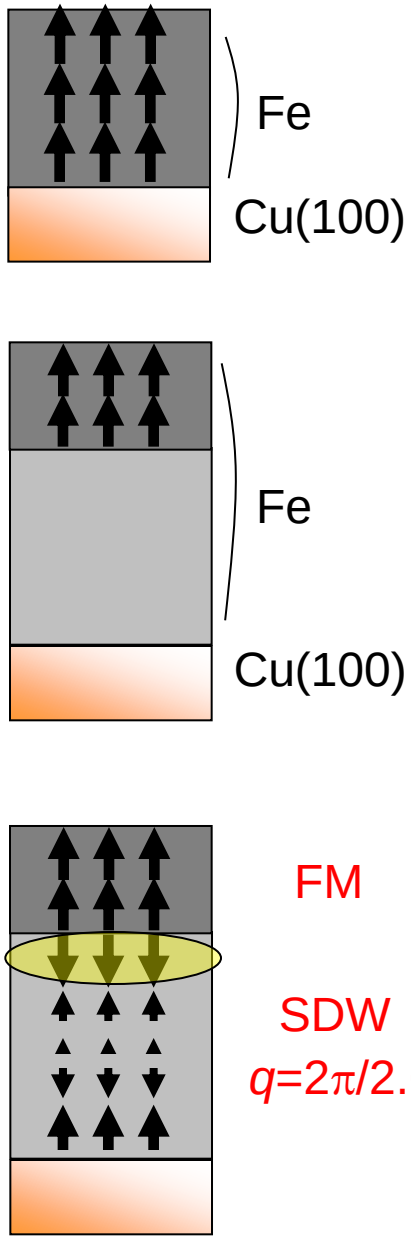

Fe/Cu(100)

>200 K

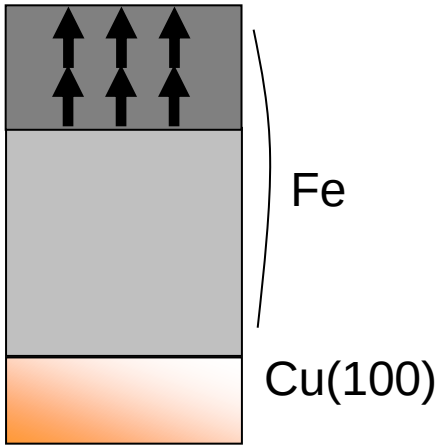

<200 K

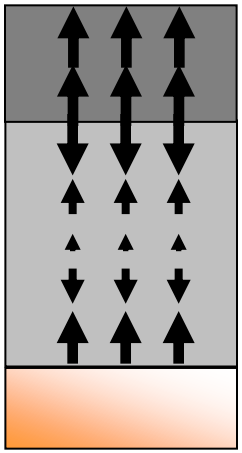

Surface (FM)

Inner layers (AFM or SDW)

No (little) magnetic interaction between Cu and interface (bottom) Fe

Fe/Ni/Cu(100)

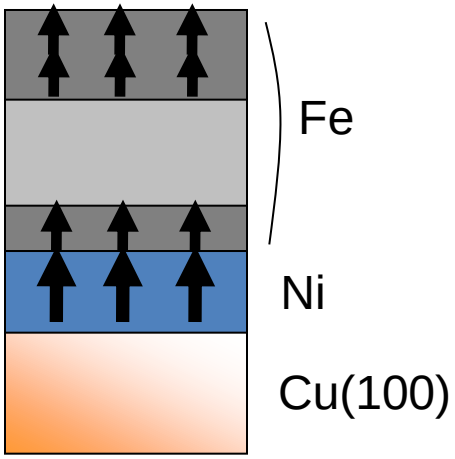

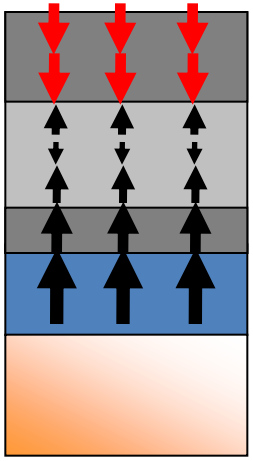

Any magnetic interaction among surface, inner layers and interface ?

Fe(x ML)/Ni(6 ML)/Cu(100)

Fe L-edge Depth-resolved XMCD

Grazing Incidence (200 K)

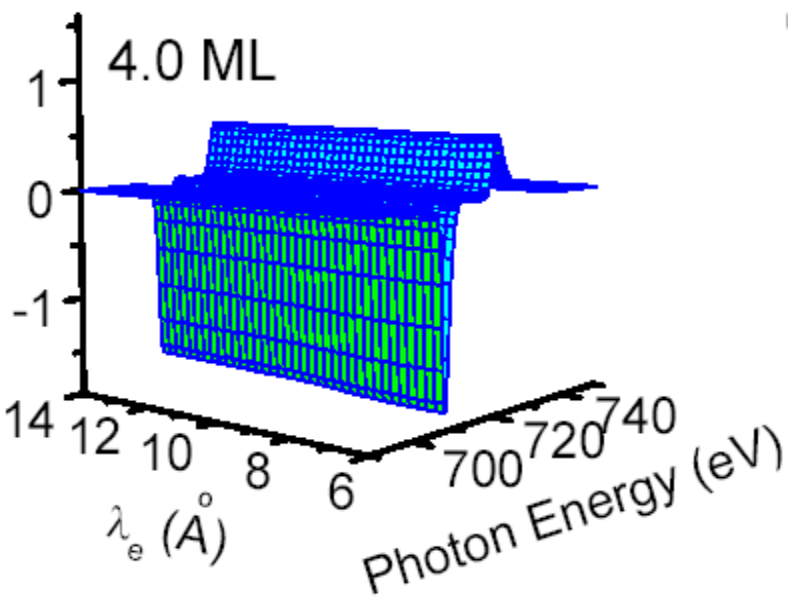

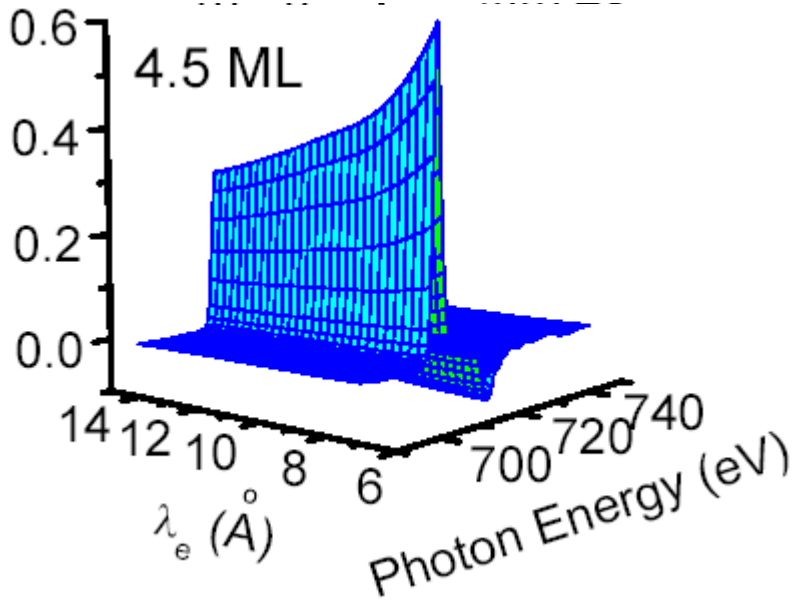

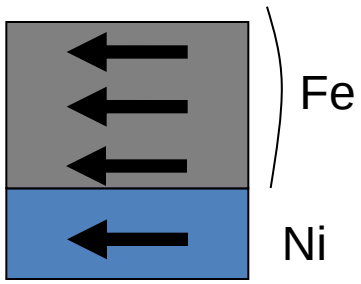

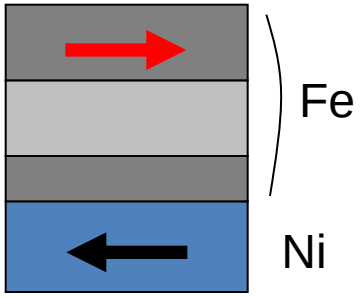

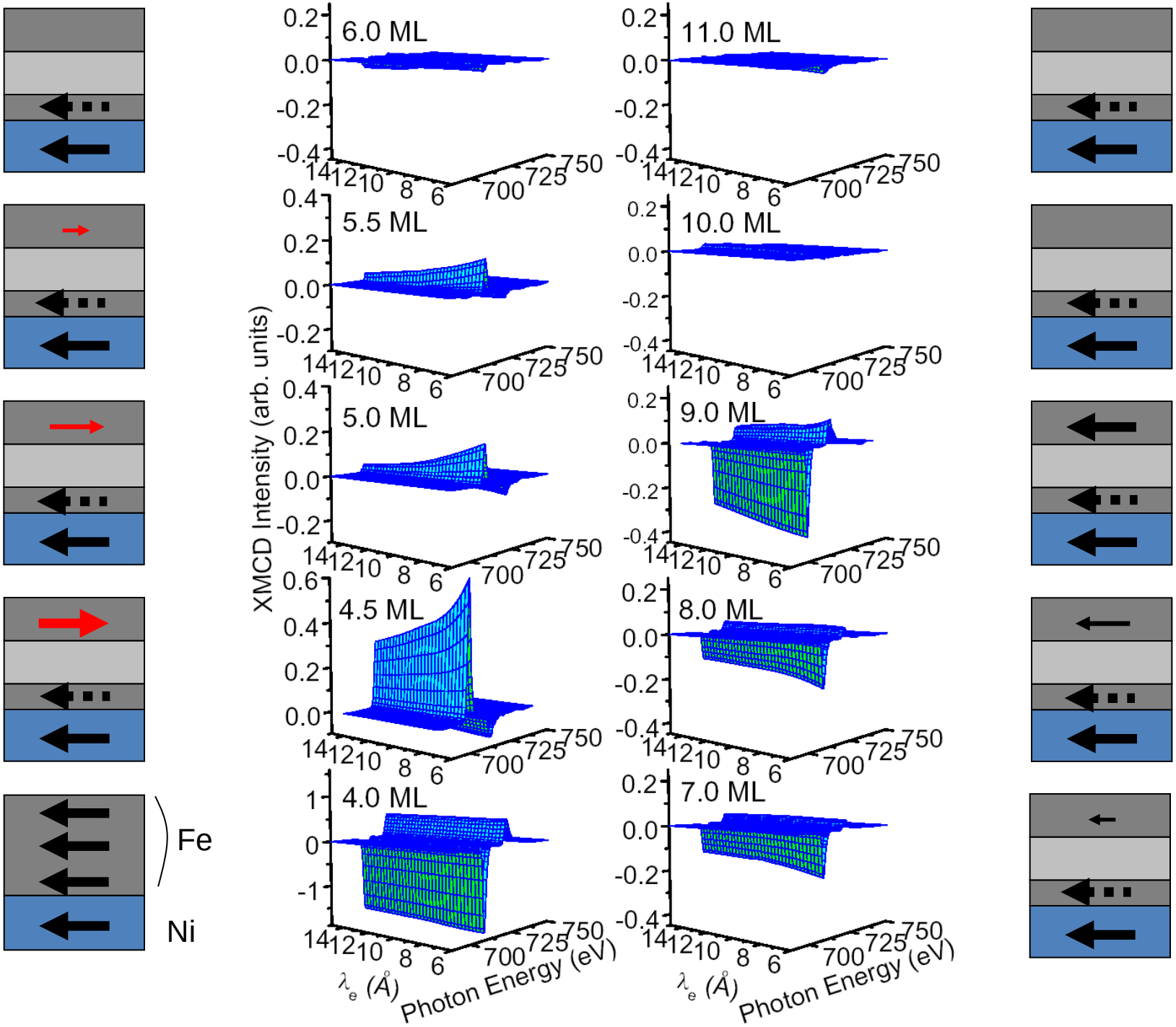
6.0 ML
11.0 ML
5.5 ML
10.0 ML
5.0 ML
9.0 ML
4.5 ML
8.0 ML
4.0 ML
7.0 ML
XMCD Intensity (arb. units)
λe (Å)
Photon Energy (eV)
Fe
Ni

Curve fitting with a three-regions model

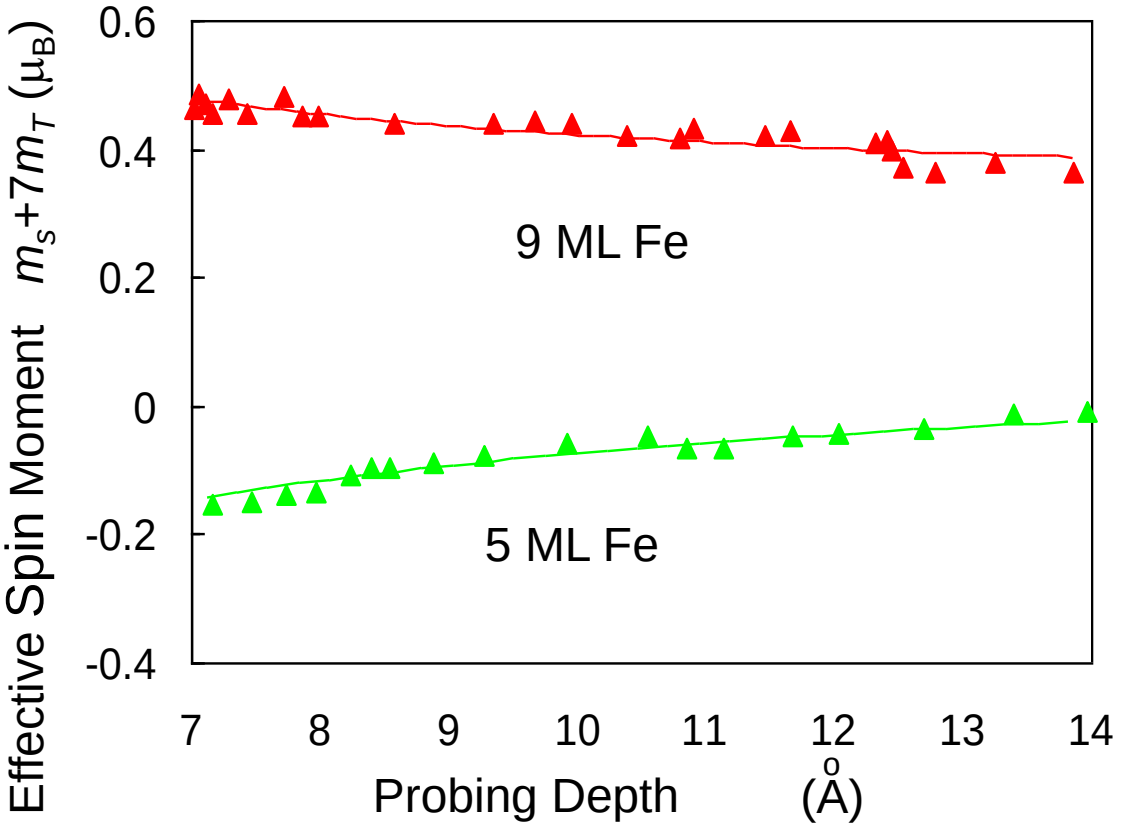

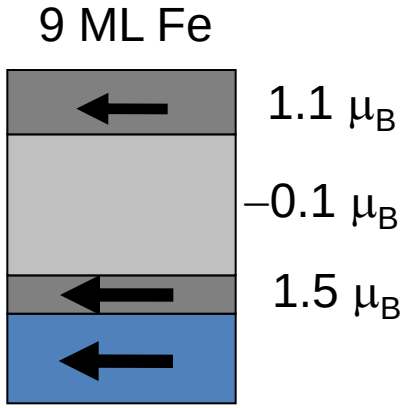

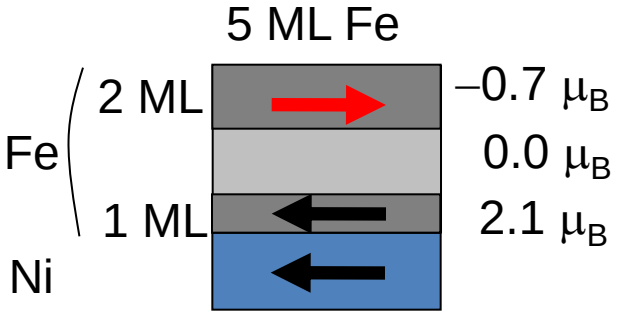

Fe thickness dependence at 200 K

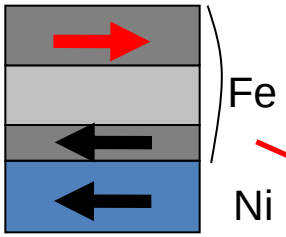

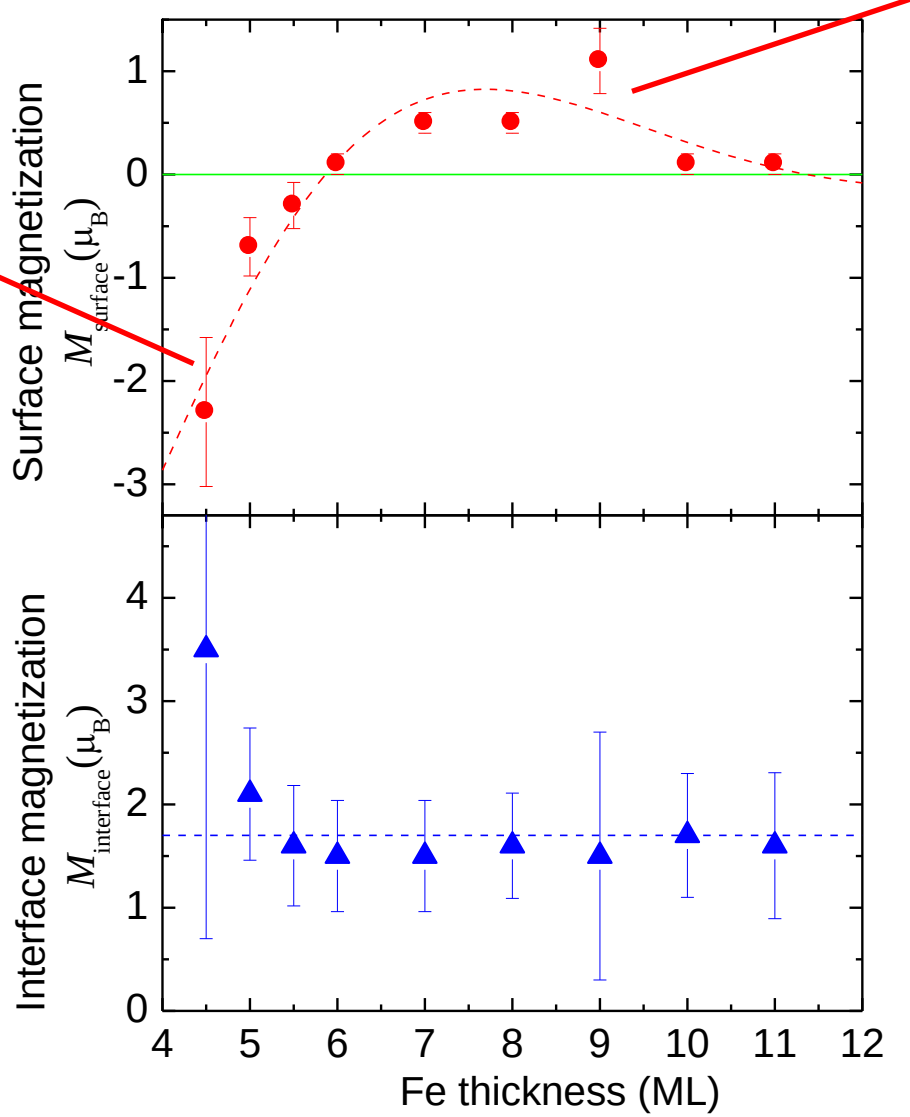

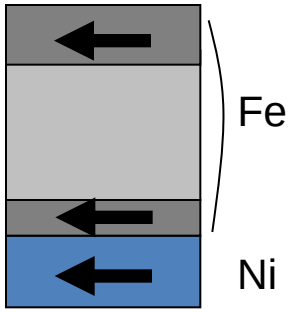

Oscillatory
surface magnetization

Positive
interface magnetization

Oscillatory
magnetic coupling
between
surface and interface

Amemiya et al., PRB 70 (2004) 195405.

Atomic structure of Ru/Co/Ru(0001) thin films

Fluorescence-yield EXAFS (Co K edge) : average over the whole film

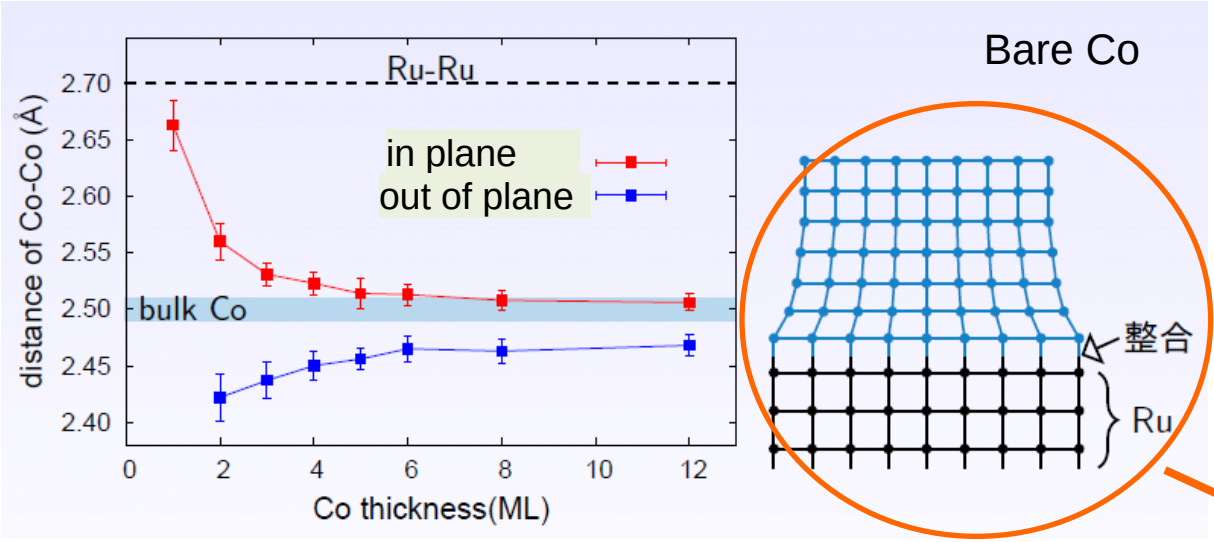

Miyawaki et al.,

PRB 80 (2009) 020408(R).

Interface Co layer is commensurate to Ru

Rapid relaxation upon further Co deposition

Effects of Ru capping

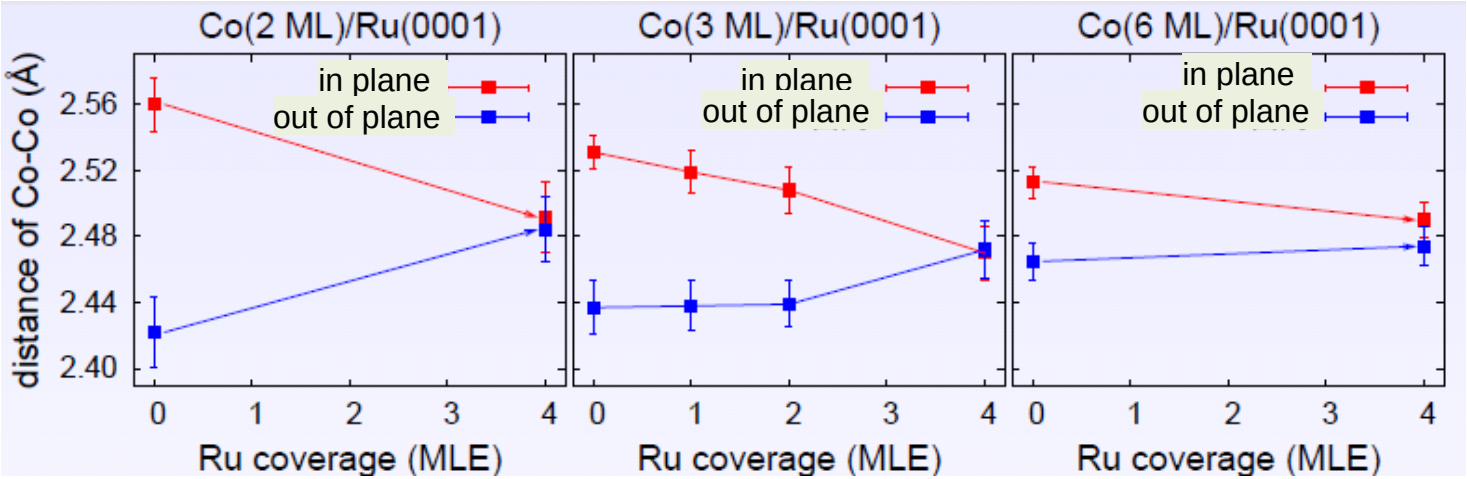

Is that true?

Relaxation of Co distortion upon Ru capping

Depth profile of atomic structure

Normal incidence: dominated by in-plane distance

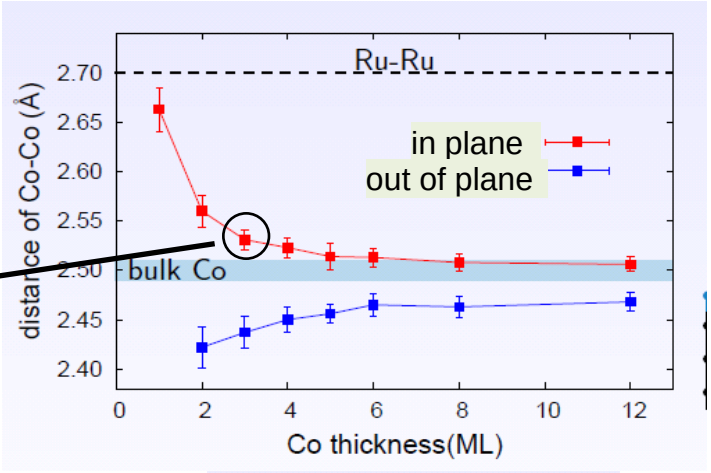

Layer-resolved EXAFS

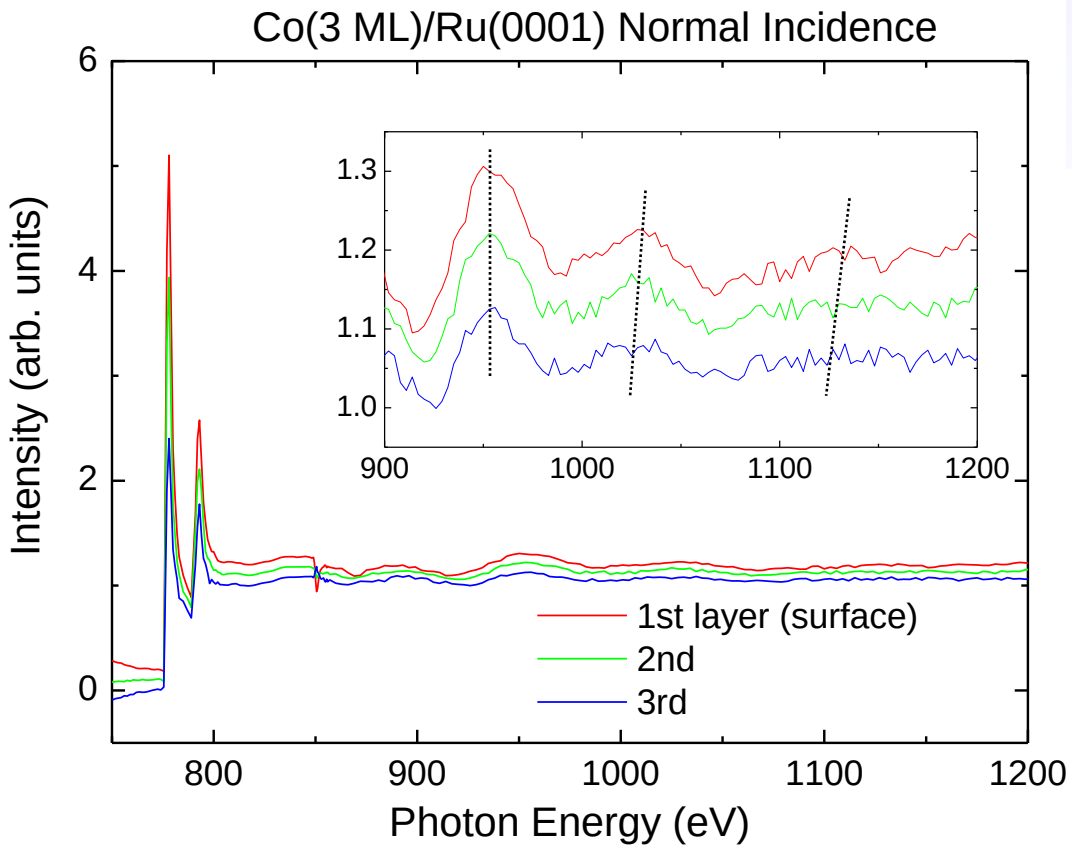

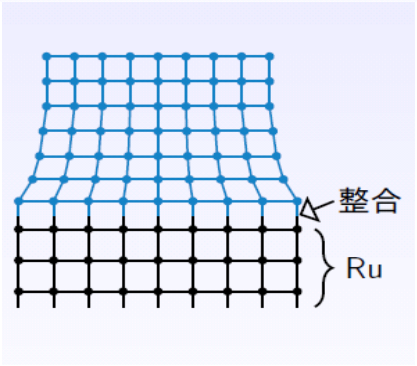

It might be true…

Surface shows longer oscillation period: shorter bond length

Depth-resolved EXAFS at grazing incidence

Longer out-of-plane bond length at surface?

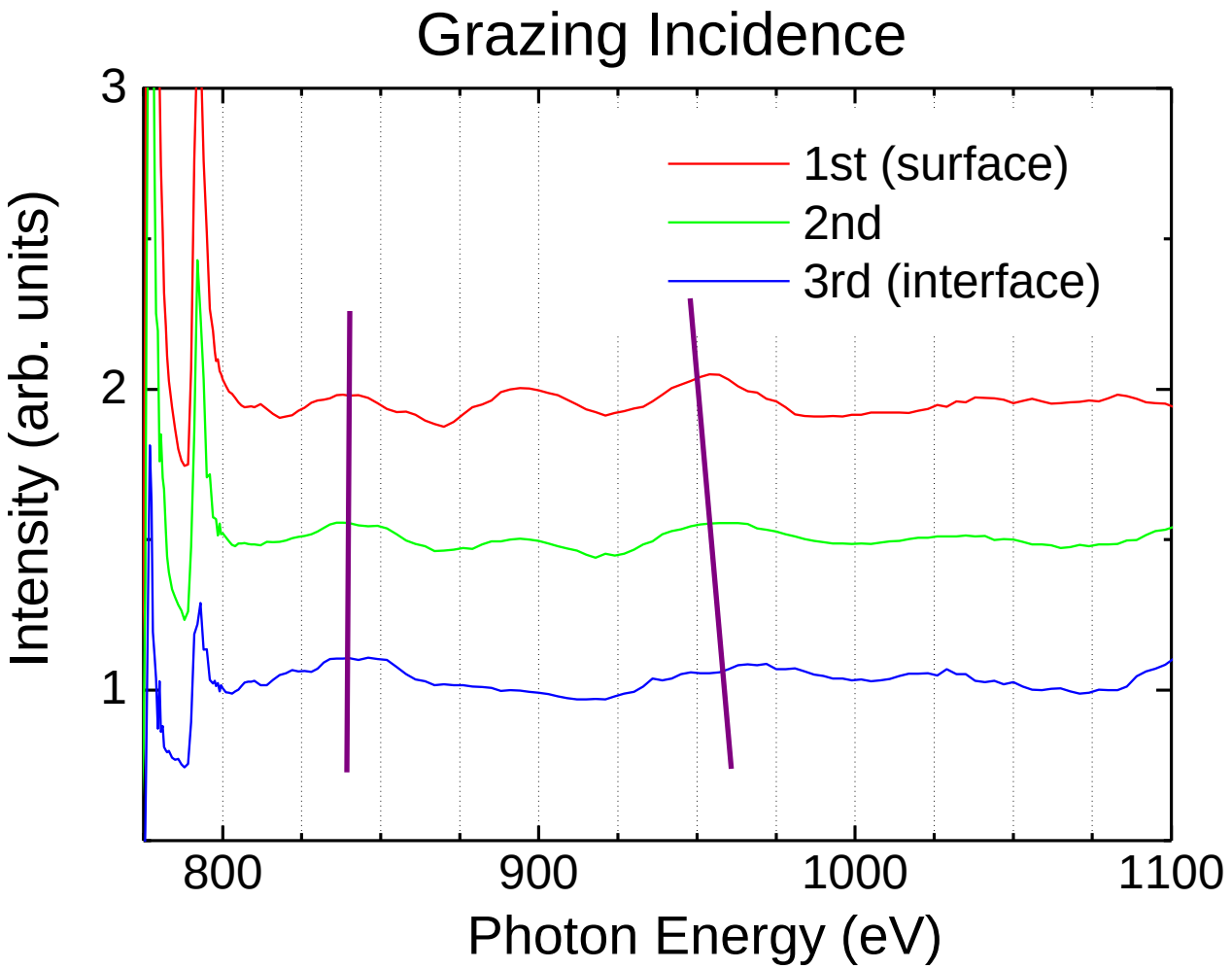

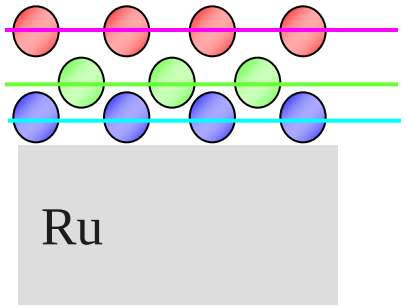

Preliminary analyses by Bayes-Turchin method

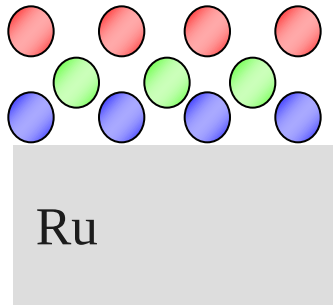

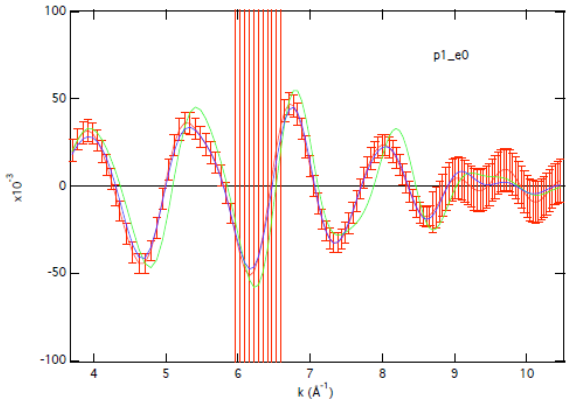

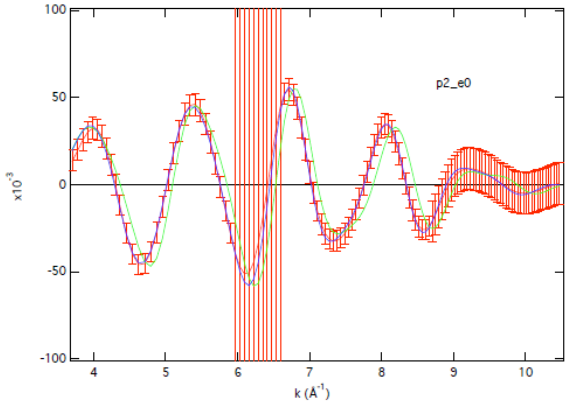

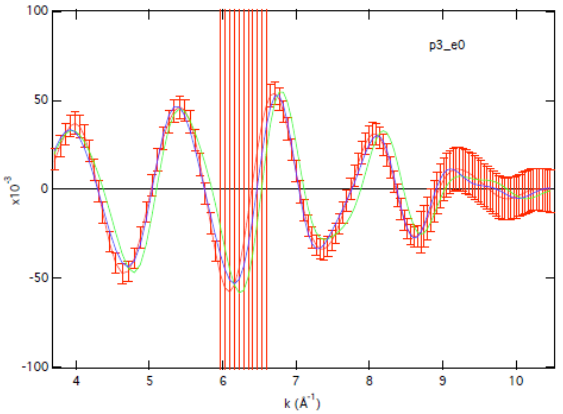

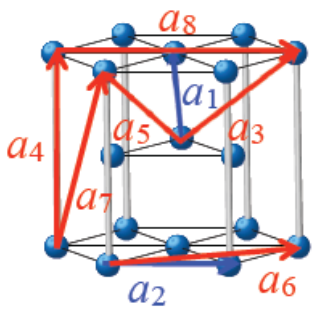

	In plane	out of plane
	2.51 Å	2.60 Å
	2.55 Å	2.52 Å
	2.55 Å	2.52 Å

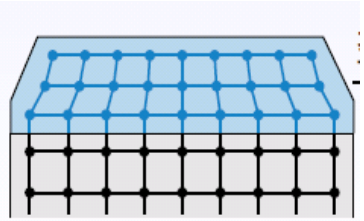

Effects of Ru capping

Normal incidence: in-plane bond length

Layer-resolved EXAFS

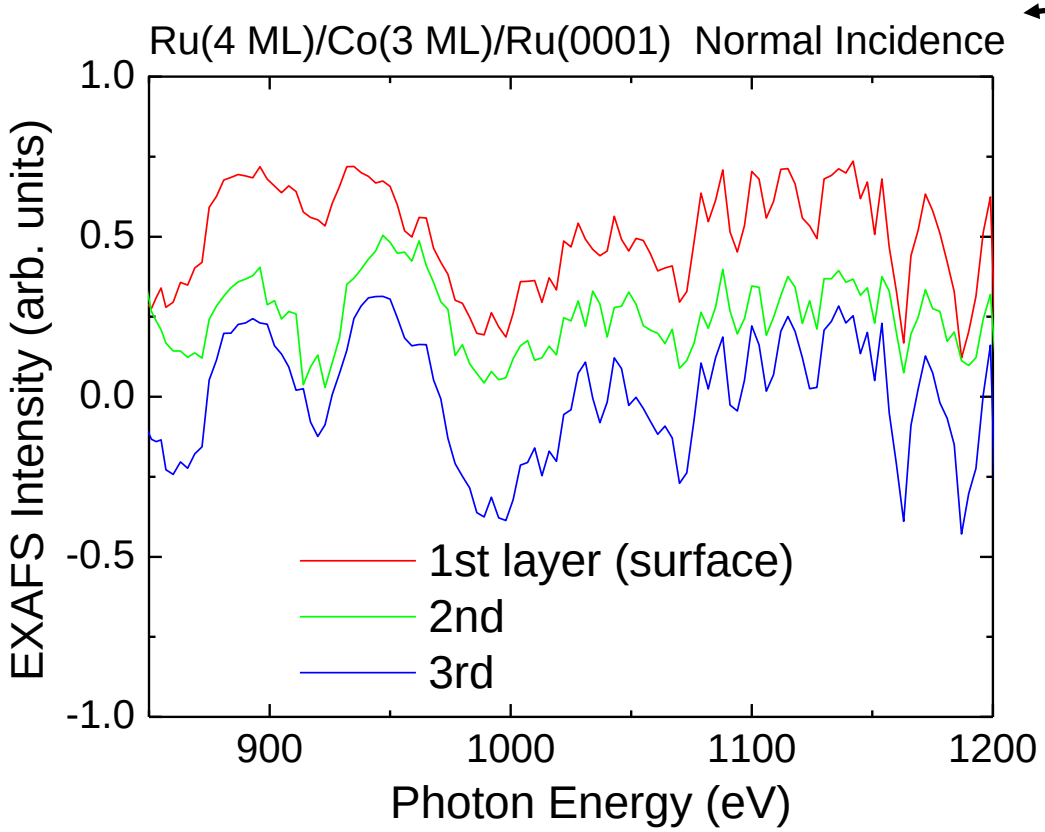

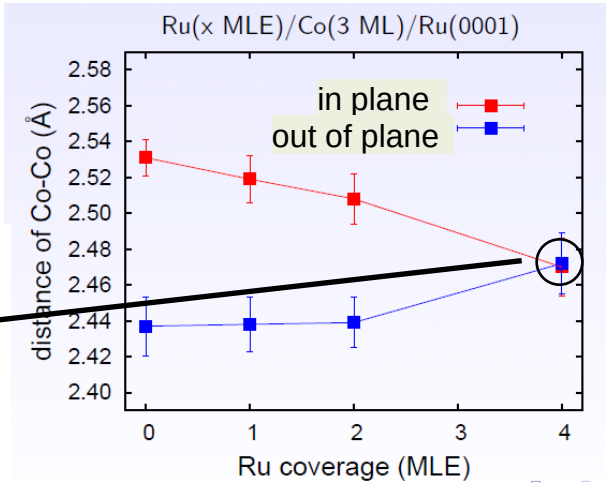

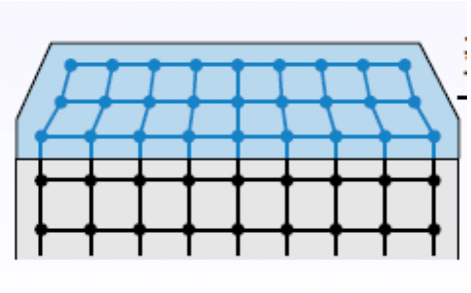

Relaxation

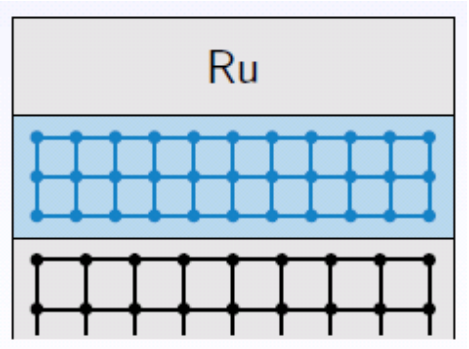

Little difference in the bond length

1. Advantages and Disadvantages of

   Soft X-ray Absorption Spectroscopy (SXAS)

2. SXAS studies on Surface and Thin films

3. Novel SXAS Techniques

   3-1. Depth-resolved XAS

   3-2. Wavelength-dispersive XAS

Development of Wavelength-dispersive XAS

XAS: Element selectivity, Chemical species determination, Structural information,…

Takes long time (~10 min/spectrum) for measurement

Possibility of "One shot" measurement.

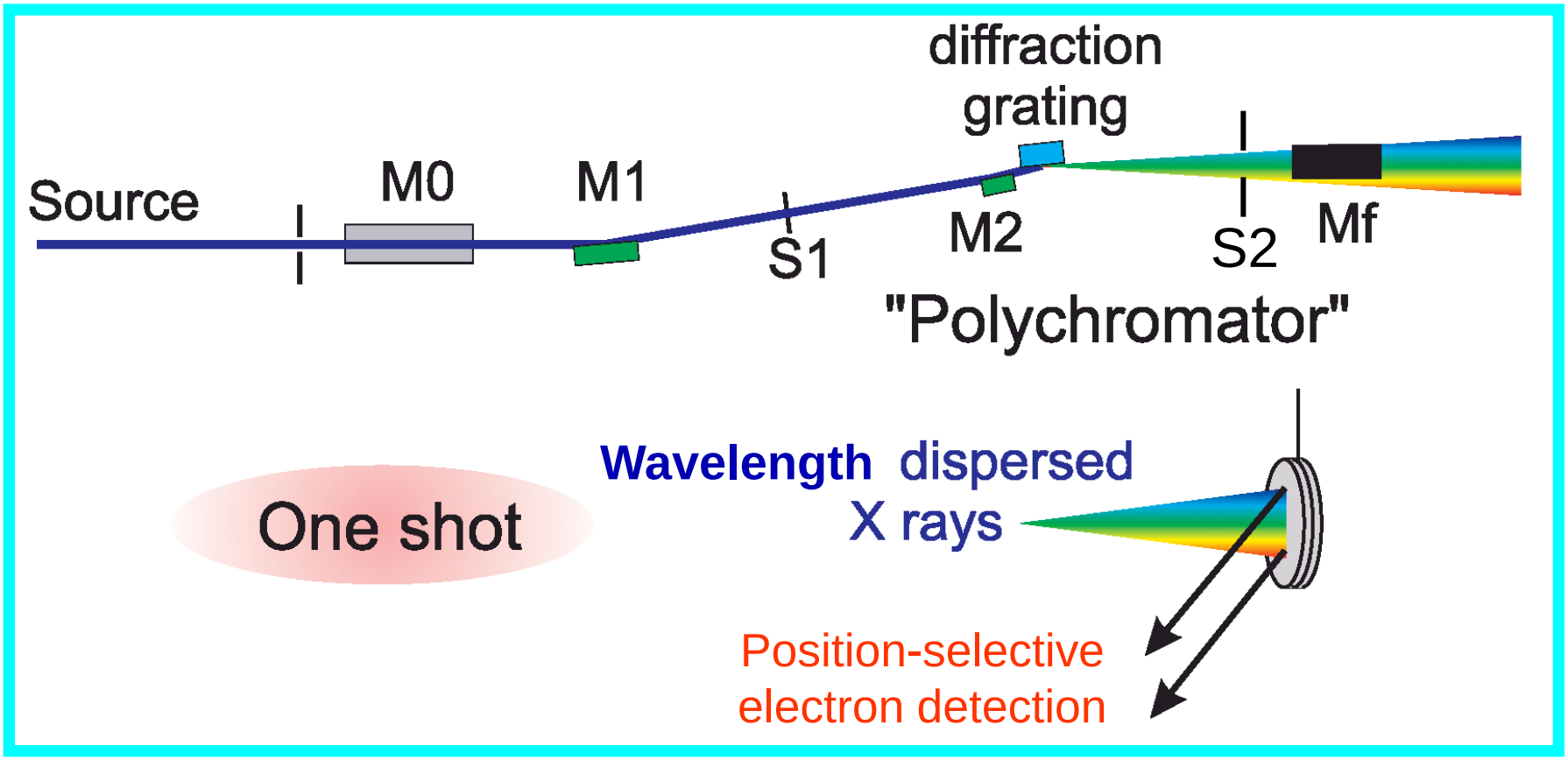

Experimental setup for wavelength-dispersive XAS

- Wavelength-dispersed X rays + Position-sensitive electron detector

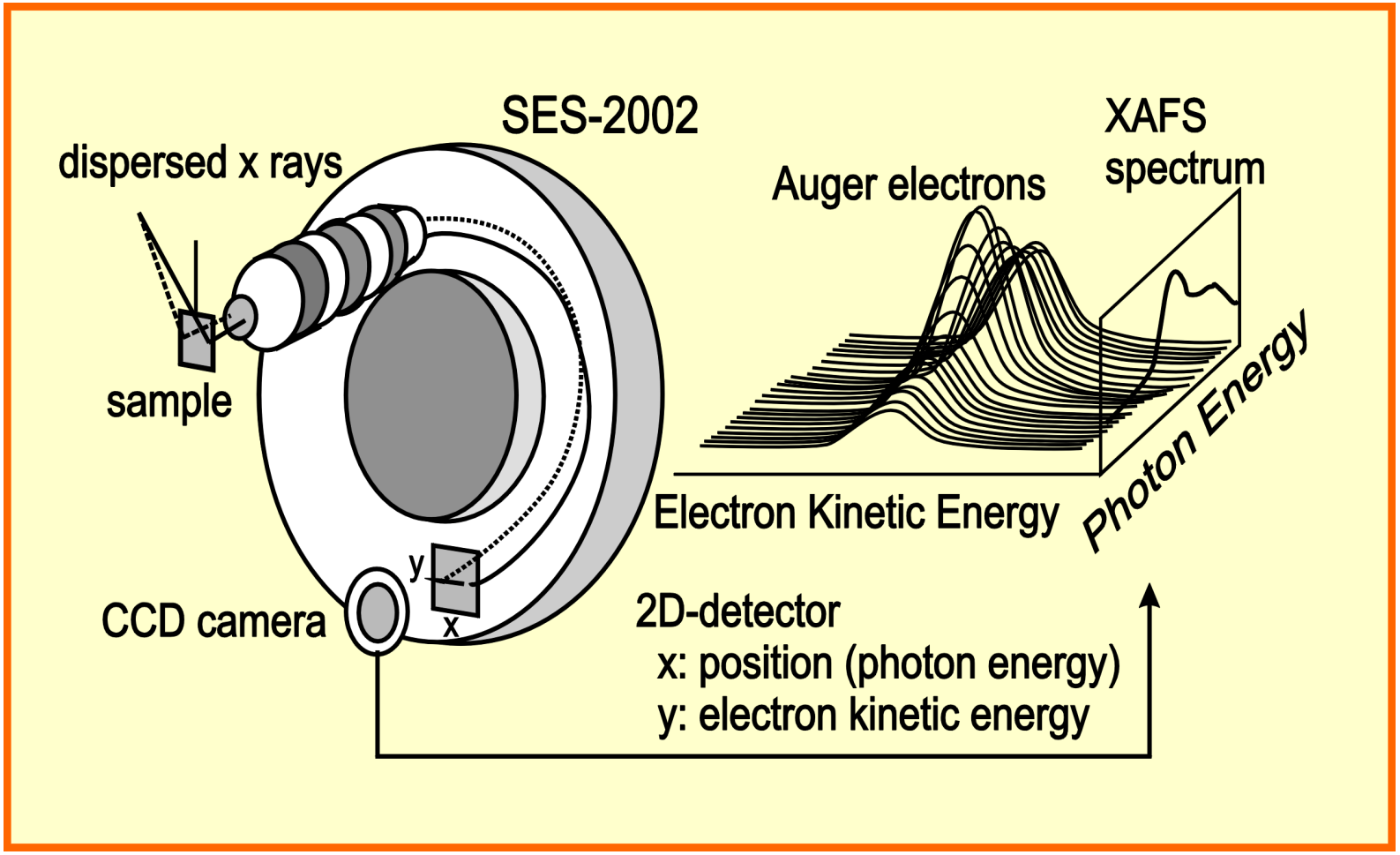

Test Measurement

Amemiya et al., Jpn. J. Appl. Phys. **40,** (2001) L718.

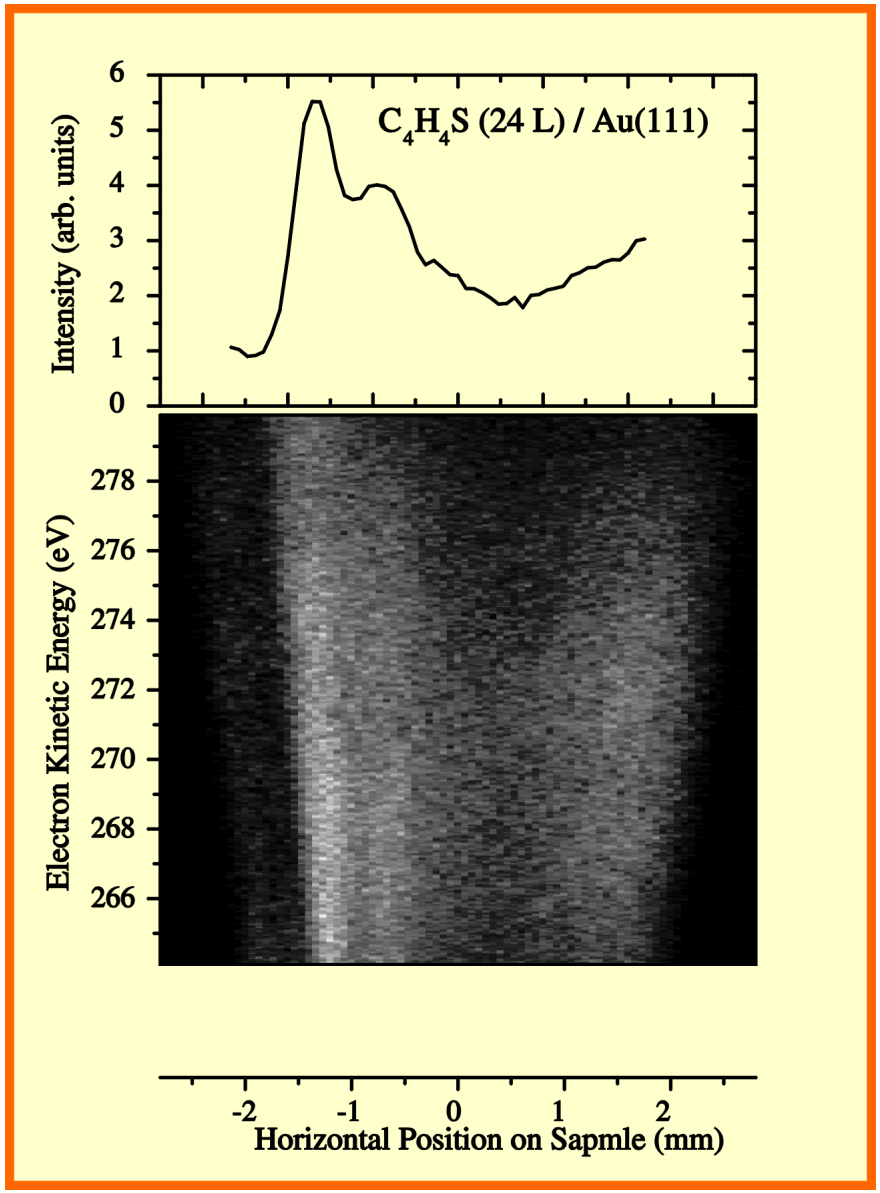

Comparison with conventional XAS

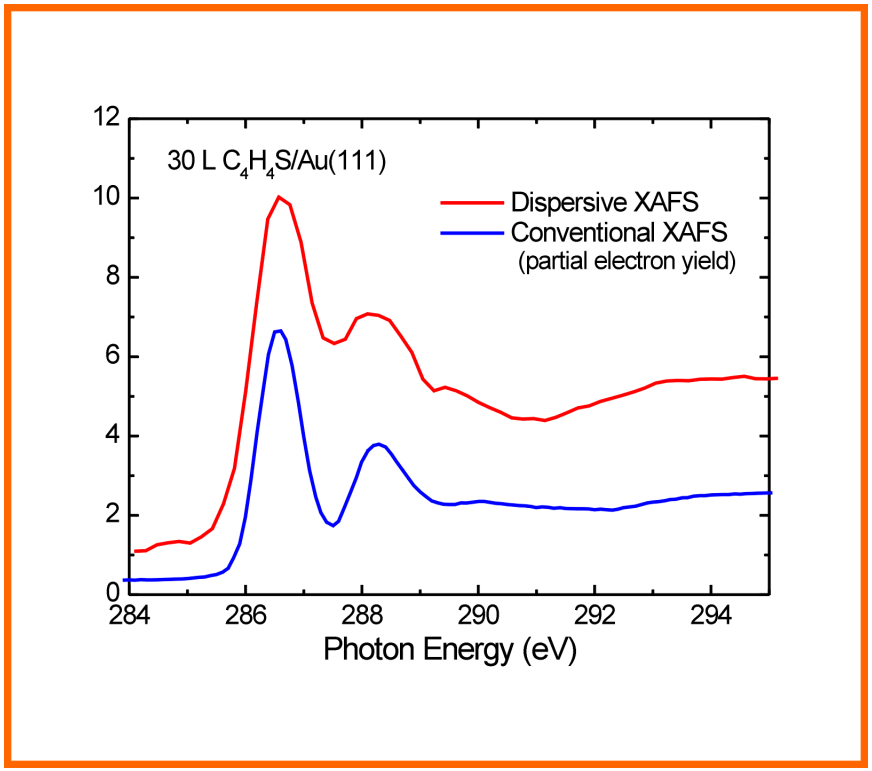

~100 times faster!

Example : C_4H_4S/Au(111)

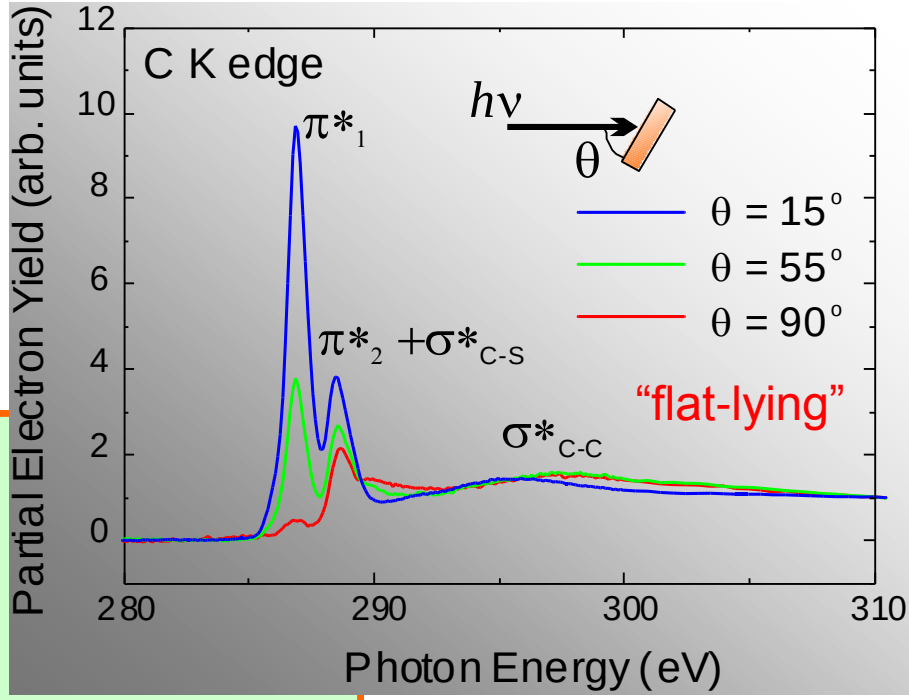

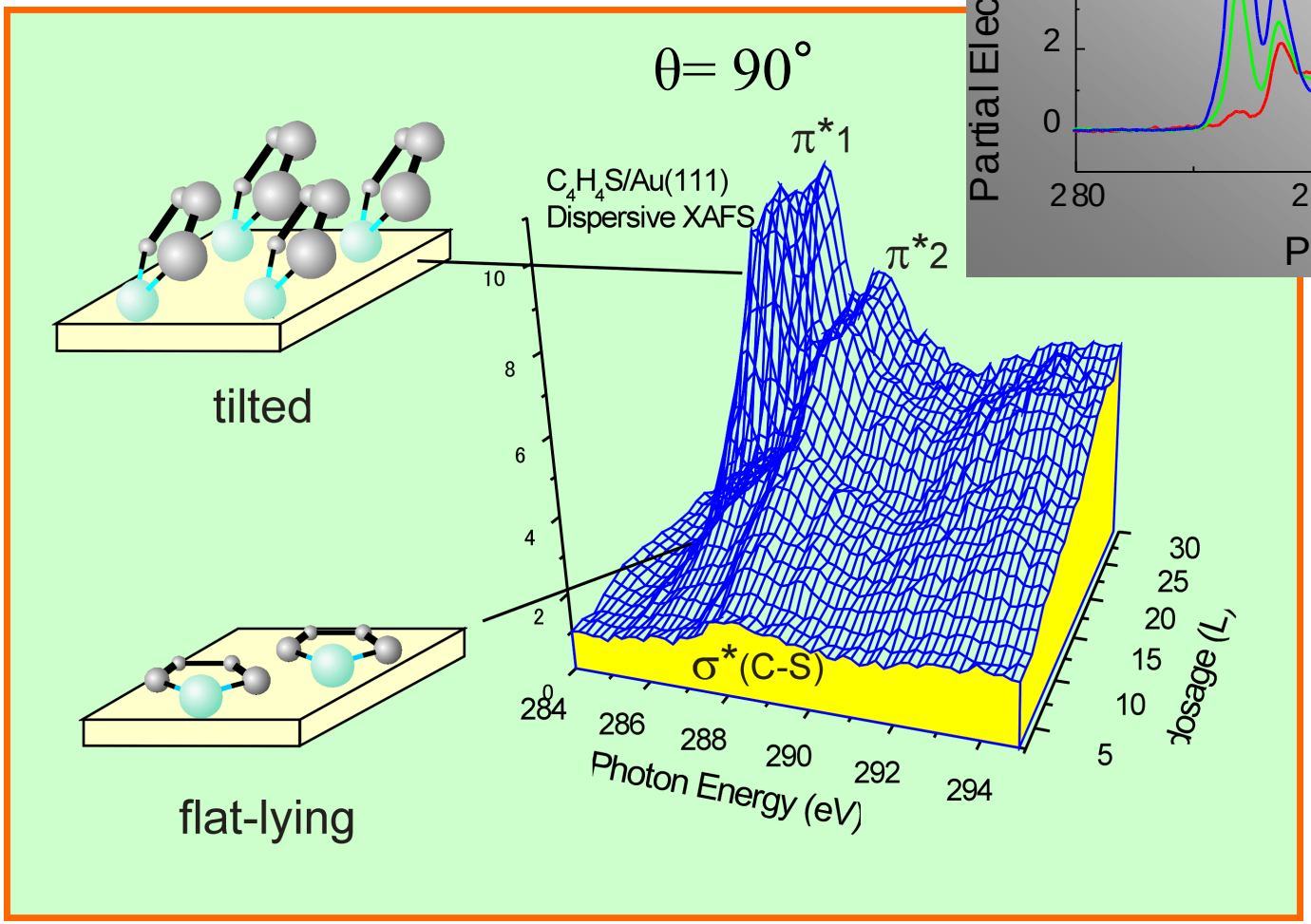

Orientation change with increasing coverage

Chemical Reaction : NO/N/Rh(111)

Nakai et al., J. Phys. Chem. B **110** (2006) 25578.

T=120 K

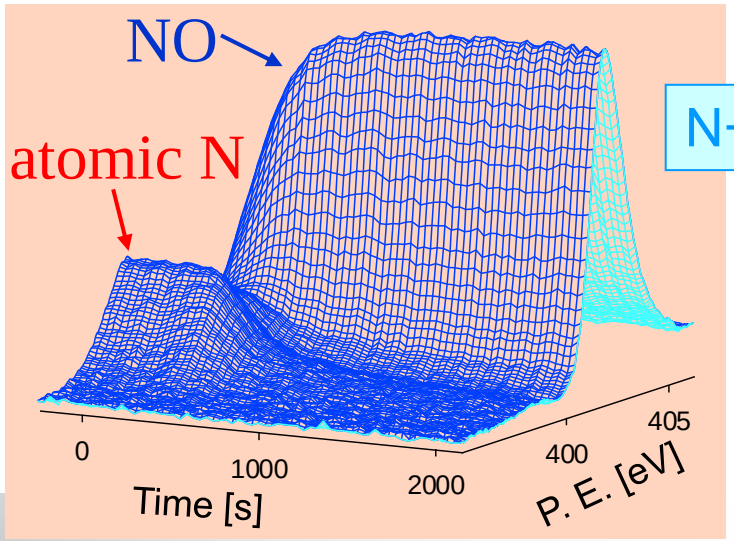

$N+NO \rightarrow N_2O\uparrow$

T=250 K

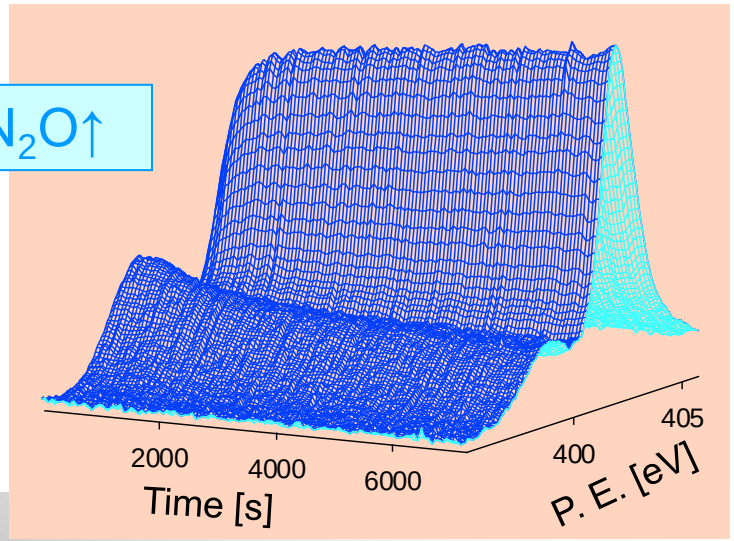

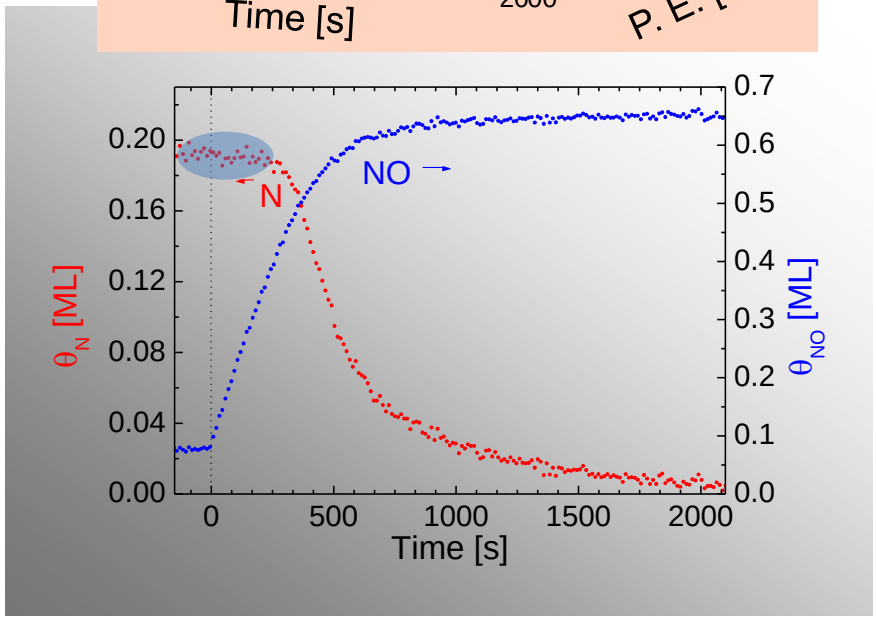

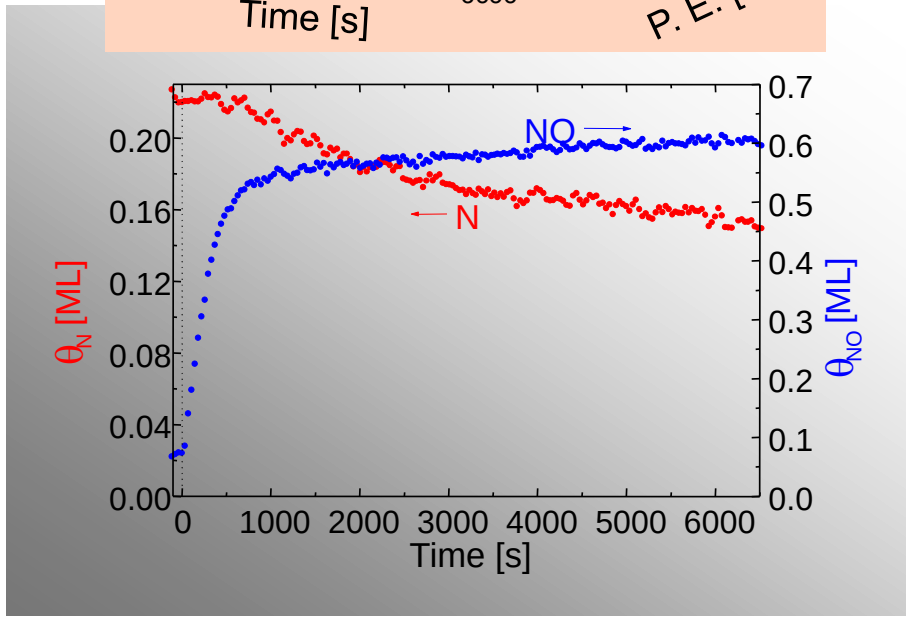

- Induction period: reaction does not start immediately
- Faster reaction at lower temperature

Lower Temperature

T=70 K, P_{NO}=5x10^{-9} Torr

Nakai et al., J. Phys. Chem. B **126** (2007) 044704.

New species

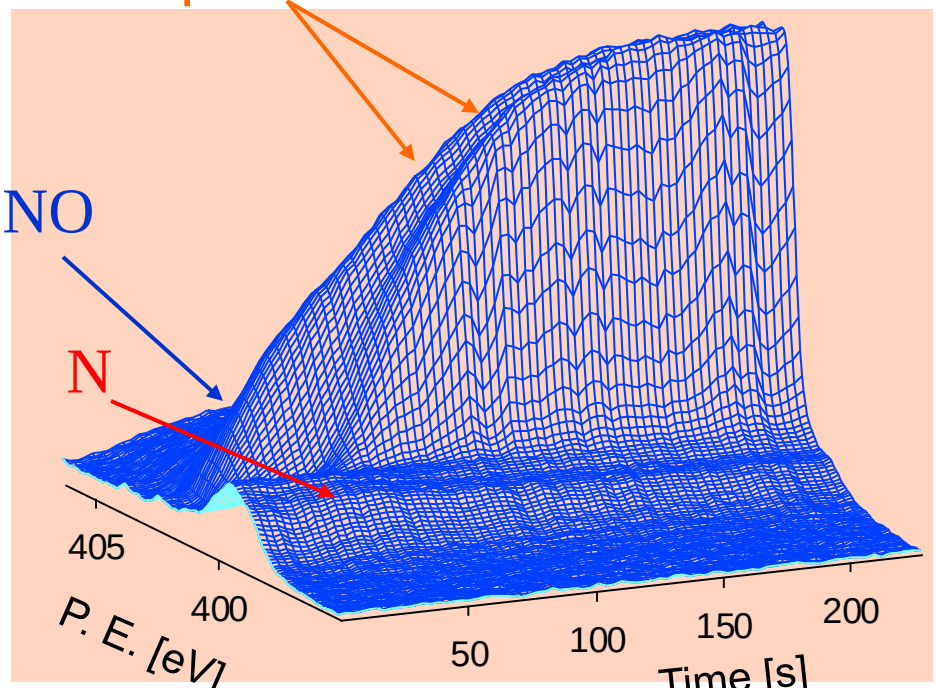

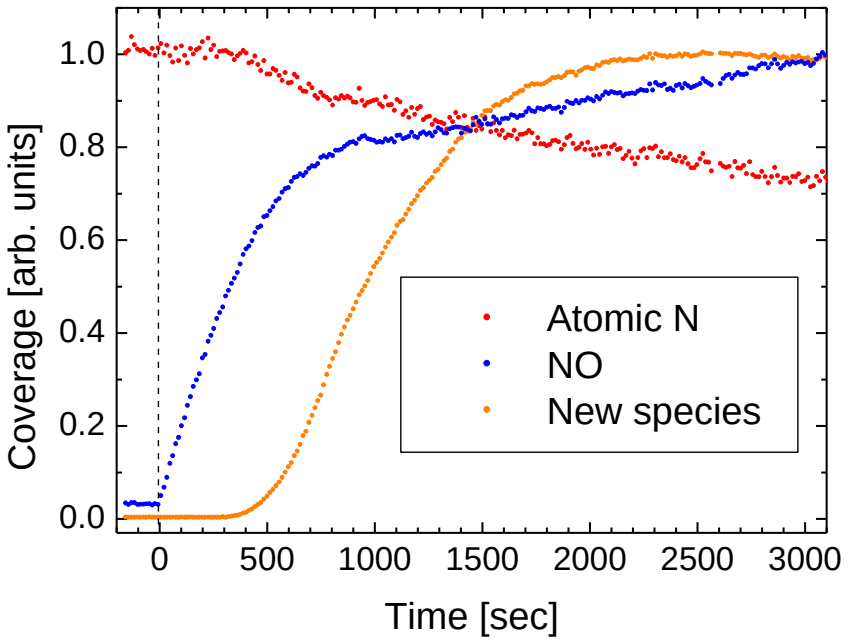

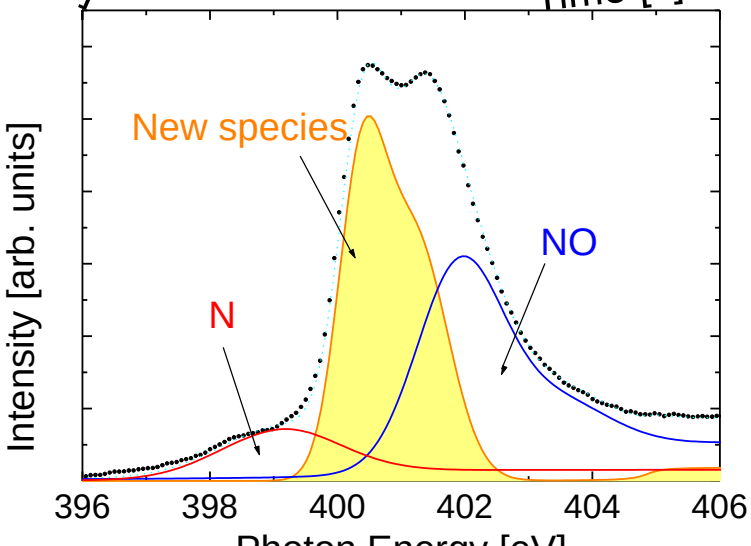

Appearance of new species

⇒ NO dimer

"New species" might be precursor.

Further Development

Undulator beamline (BL-16A)
Video rate (~30 Hz)

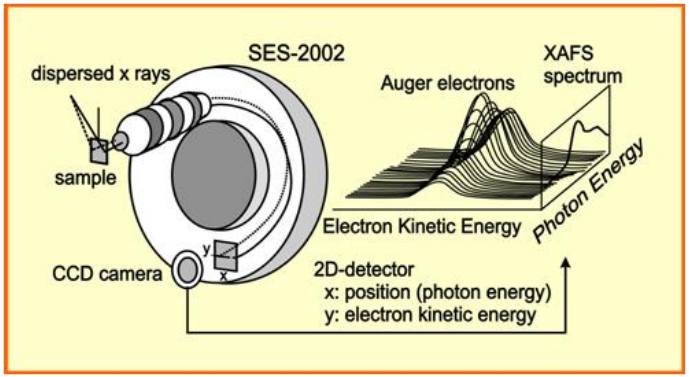

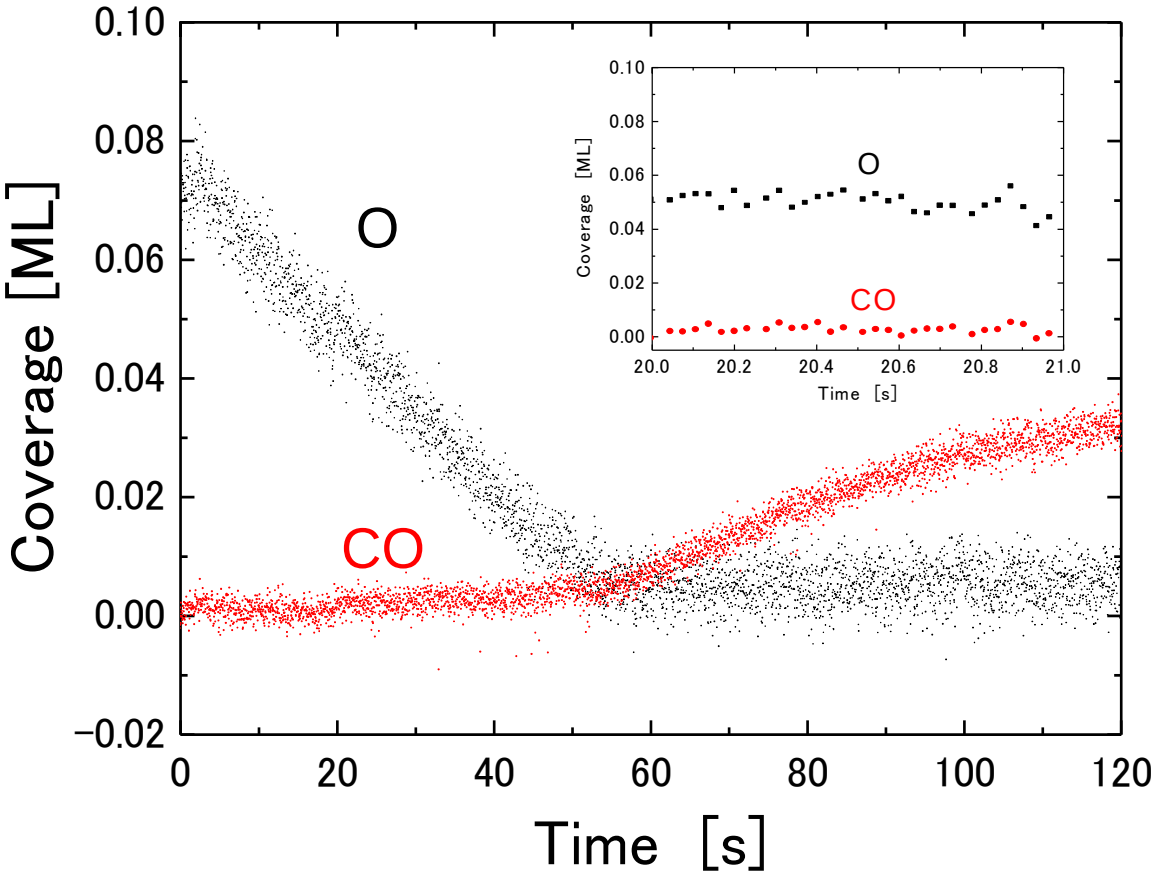

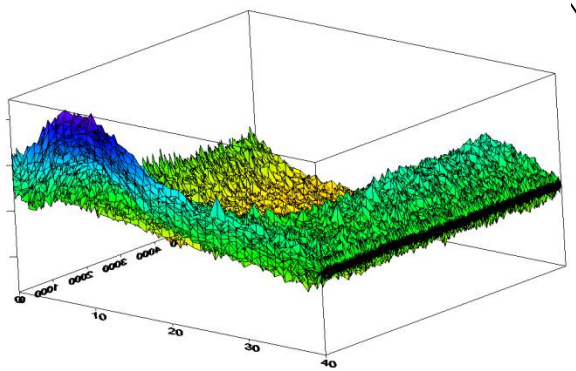

400 K

Experimental conditions

O : p(2x2)

CO: $P_{CO} = 1 \times 10^{-8}$ Torr

acquisition time:
33 ms/spectrum

Thank you for your attention!